Cancer Cell
Article

Bile Acid and Inflammation Activate Gastric Cardia Stem Cells in a Mouse Model of Barrett-Like Metaplasia

Michael Quante,[1,2,10,*] Govind Bhagat,[2,3] Julian A. Abrams,[1,2] Frederic Marache,[1,2] Pamela Good,[1,2] Michele D. Lee,[1,2] Yoomi Lee,[4] Richard Friedman,[5] Samuel Asfaha,[1,2] Zinaida Dubeykovskaya,[1,2] Umar Mahmood,[7] Jose-Luiz Figueiredo,[8] Jan Kitajewski,[2,6] Carrie Shawber,[2,6] Charles J. Lightdale,[1,2] Anil K. Rustgi,[9] and Timothy C. Wang[1,2,*]

[1]Division of Digestive and Liver Diseases, Department of Medicine
[2]Herbert Irving Comprehensive Cancer Center
[3]Department of Pathology and Cell Biology
[4]Division of Hematology and Oncology, Department of Medicine
[5]Department of Biomedical Informatics
[6]Department of Pathology, Obstetrics and Gynecology
Columbia University Medical Center, New York, NY 10032, USA
[7]Nuclear Medicine and Molecular Imaging
[8]Center for Systems Biology
Harvard Medical School and Massachusetts General Hospital, Boston, MA 02114, USA
[9]Division of Gastroenterology, Department of Medicine and Genetics, Abramson Cancer Center, University of Pennsylvania, Philadelphia, PA 19104, USA
[10]II. Medizinische Klinik, Klinikum rechts der Isar, Technische Universität München, 81675 Munich, Germany
*Correspondence: michael.quante@lrz.tum.de (M.Q.), tcw21@columbia.edu (T.C.W.)
DOI 10.1016/j.ccr.2011.12.004

SUMMARY

Esophageal adenocarcinoma (EAC) arises from Barrett esophagus (BE), intestinal-like columnar metaplasia linked to reflux esophagitis. In a transgenic mouse model of BE, esophageal overexpression of interleukin-1β phenocopies human pathology with evolution of esophagitis, Barrett-like metaplasia and EAC. Histopathology and gene signatures closely resembled human BE, with upregulation of TFF2, Bmp4, Cdx2, Notch1, and IL-6. The development of BE and EAC was accelerated by exposure to bile acids and/or nitrosamines, and inhibited by IL-6 deficiency. Lgr5^{+} gastric cardia stem cells present in BE were able to lineage trace the early BE lesion. Our data suggest that BE and EAC arise from gastric progenitors due to a tumor-promoting IL-1β-IL-6 signaling cascade and Dll1-dependent Notch signaling.

INTRODUCTION

Esophageal adenocarcinoma (EAC) has been linked to chronic inflammation of the esophagus and its incidence has increased by more than 500% since the 1970s (Corley et al., 2009) despite powerful acid suppressant medications (proton pump inhibitors) and a decline in the prevalence of *Helicobacter pylori* in the United States and Europe. The main risk factor for EAC is Barrett esophagus (BE), involving a progression from BE to low-grade/high-grade dysplasia (Falk, 2002). The precise origin of both EAC and BE has been difficult to discern in part because of the absence of useful experimental model systems that are genetically based.

BE has been attributed primarily to gastroesophageal reflux disease (GERD), leading to chronic inflammation of the esophagus. The link between inflammation and cancer is well established (Grivennikov et al., 2010); in particular, elevated IL-6 has been identified as a key mediator of tumorigenesis in murine models of cancer (Grivennikov and Karin, 2008). IL-1β, a pleiotropic pro-inflammatory cytokine upstream of IL-6 and

Significance

Using a transgenic mouse model of BE and EAC, that closely resembles the human disease, insights into the pathogenesis of BE are provided. A gastric cardia progenitor cell lineage appears to be activated by bile acid-induced and IL-1β- and IL-6-dependent inflammation, inducing migration into the distal esophagus where it gives rise to columnar-like metaplasia and dysplasia. Activated Notch signaling appears to regulate differentiation of the cardia progenitor into intestinal-type columnar cells instead of goblet cells, and is associated with a malignant transformation in mice and humans. Our findings challenge the common paradigms regarding the pathogenesis of BE and EAC.

TNF-α signaling cascades, has been demonstrated to induce tumorigenesis of the mouse stomach (Tu et al., 2008). IL-1β is overexpressed in BE, and clinical studies have suggested that polymorphisms in the *IL-1β* gene cluster are associated with BE (Fitzgerald et al., 2002; Gough et al., 2005; O'Riordan et al., 2005).

BE is defined as replacement of the stratified squamous epithelium in the distal esophagus with a metaplastic, intestinal-like columnar epithelium (Spechler et al., 2010). Whereas attention in the past has been focused on goblet cells (i.e., classical intestinal metaplasia [IM]) as the primary marker for BE, the recent change in the definition to include nongoblet, columnar lined esophagus ([CLE], resembling intestinal and cardia metaplasia) was made to acknowledge the more variable histologic presentation of BE. A major unanswered question that has been debated for decades, is whether the BE cell of origin derives from transdifferentiation of the esophageal squamous epithelium (Yu et al., 2005), or originates rather from a progenitor cell in the esophagus (Kalabis et al., 2008), the esophageal submucosal glands (Leedham et al., 2008), residual embryonic cells located at the squamocolumnar junction (Wang et al., 2011), or, as early investigators proposed, the gastric cardia (Allison and Johnstone, 1953; Barbera and Fitzgerald, 2010; Hamilton and Yardley, 1977; Nakanishi et al., 2007). However, prior to the development of IM, a regenerative intestinal-like columnar cell lineage appears in the esophagus that expresses TFF2, KRT8, KRT20, NOTCH, and CDX2 (Hanby et al., 1994; Menke et al., 2010; Stairs et al., 2008; Tatsuta et al., 2005). It is crucial to identify the progenitors responsible for BE, given the preneoplastic nature of the lesion.

Until recently, the primary animal model used to study BE has been a rat model comprising esophagojejunostomy that induces gastroduodenal reflux (Fein et al., 1998; Li and Martin, 2007). The observation that duodenesophageal reflux induces EAC in rats points to the importance of refluxed duodenal contents in the pathogenesis of BE. Bile acids, particularly unconjugated bile acids such as deoxycholate (DCA) that induce DNA damage, are one component of gastroduodenal reflux that have been linked strongly to the development of BE. Reflux injury in the esophagus results in chronic inflammation with upregulation of numerous cytokines, such as IL-1β, IL-6, and IL-8, that might contribute to the metaplastic and dysplastic conversion of BE (Fitzgerald et al., 2002). Here, we aimed to utilize a model of Barrett-like metaplasia, involving overexpression of IL-1β, to provide insights into the origins of Barrett esophagus.

RESULTS

Interleukin-1β Overexpression in the Mouse Esophagus Induces Esophagitis, Barrett-Like Metaplasia, and Neoplasia

To understand the pathogenesis of BE and EAC we generated a model of chronic esophageal inflammation, inserting the modified human *IL-1β* cDNA (Björkdahl et al., 1999) downstream of an Epstein-Barr virus (ED-L2) promoter that targets the oral cavity, esophagus, and squamous forestomach (Figure S1A available online) (Nakagawa et al., 1997). In two founder lines we observed high (Line 1) and low levels (Line 2) of specific esophageal (and forestomach) hIL-1β mRNA and protein expression (Figures 1A and 1B) that correlated with upregulated IL1-receptor-antagonist (IL1ra), indicative of IL-1 receptor signaling (Figure 1C). No hIL-1β mRNA and protein expression was observed in the glandular stomach or elsewhere (Figures 1A and 1D). *L2-IL-1β* mice developed splenomegaly (Figure S1C) that correlated with age dependent IL-1β expression levels (Figure 1B), consistent with a systemic inflammatory reaction and at least 10-fold elevated ($p < 0.05$) circulating levels of IL-1β, TNFα (Figure S1D), and IL-6 (Figure 1D).

The esophagus and squamous forestomach in the low and high expressing *L2-IL-1β* mice were markedly thickened with a mixed acute and chronic inflammatory infiltrate compared to age-matched wild-type (WT) mice (Figure S1B). However, the major histopathological changes in *L2-IL-1β* mice occurred at the squamocolumnar junction (SCJ), an anatomical location where the squamous and gastric columnar epithelium meet (Figure 1E) and where the esophagus enters the stomach. Compared to the human SCJ, the mouse esophagus enters the stomach at the midpoint of the lesser curvature of the stomach, at the junction between the glandular stomach and squamous forestomach, forming a SCJ that traverses the entire stomach and resembles the Z line in the human esophagus (Figure S1E). To determine whether the L2-IL-1β mice develop metaplasia resembling human BE, histological evaluation was performed on sagittal sections through the esophagus and stomach (Figure S1E, yellow line). Based upon previously described criteria (Fox et al., 2000), a histopathological scoring system for the mouse SCJ was developed. In 100% (10/10) of the 6-month-old *L2-IL-1β* mice, we observed moderate inflammation and profound epithelial hyperplasia (Figure 1F) that was never observed in age-matched WT mice. Proliferation was increased significantly in the esophageal basal compartment (Figure 2A).

In *L2-IL-1β* mice that were 12–15 months of age, 90% (9/10) developed severe columnar metaplasia (Figures 1E and 1F) with mucus producing (*Muc5ac*$^+$, PAS$^+$) cells (Figure 2A) at the SCJ, similar to human BE. Although classical goblet cells were not observed in *L2-IL-1β* mice, the mucus producing columnar cell types observed were consistent with Barrett-like metaplasia. *Tff2*, a marker for metaplasia in human BE (Van De Bovenkamp et al., 2003; Warson et al., 2002), and also an oxyntic progenitor cell marker in the gastric corpus (Quante et al., 2010), was not expressed in the WT esophagus but was upregulated above the SCJ of *L2-IL-1β* mice harboring metaplasia but not in dysplasia (Figure 2A). Electron microscopy studies revealed nearly identical ultrastructural features (columnar cell type, microvilli, granules, mucins) in human and mouse BE (Figure 2B). At 20–22 months of age, 20% (2/9) of *L2-IL-1β* mice developed high-grade dysplasia (HGD) or intramucosal EAC (Figures 1E–1G). These lesions were grossly visible within the distal end of the esophagus (Figure 1G) and were associated with significant weight loss (28% ± 4%, $p < 0.05$; data not shown). During this stepwise progression to cancer, we observed a gradual increase in αSMA$^+$ stromal myofibroblasts (Figure 2A) and increasing stroma global hypomethylation (Figure S2) in BE and HGD compared to WT, consistent with other models of inflammation-induced cancer (Jiang et al., 2008). Although hypomethylation was prominent in the stroma, we could not exclude (and

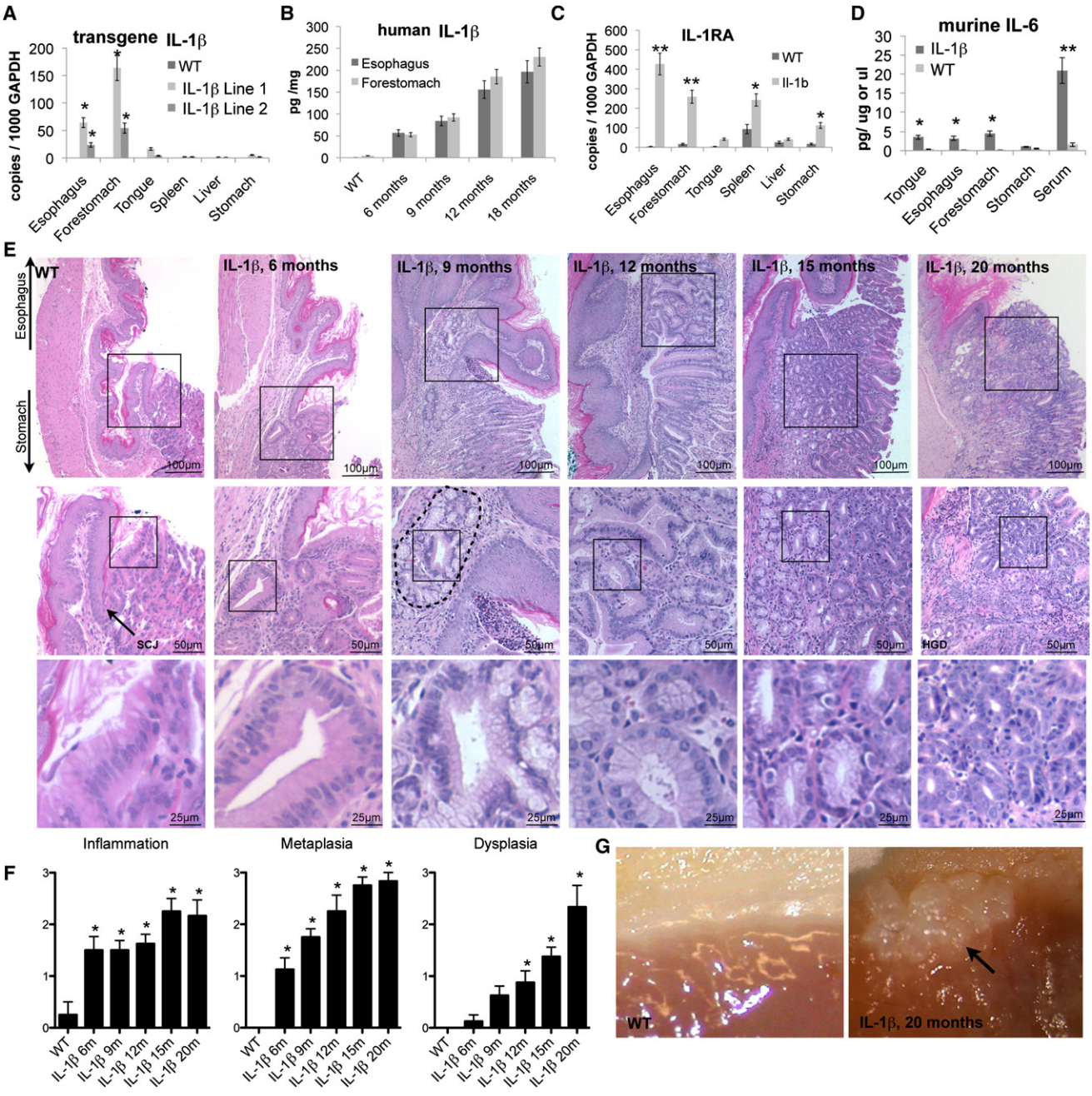

Figure 1. Overexpression of IL-1β-Induced Chronic Inflammation in the Murine Esophagus and Stepwise Development of Metaplasia and Dysplasia at the SCJ

(A) mRNA expression (RT-qPCR) in different organs of 3-month-old two founder *L2-IL-1β*-lines.

(B) ELISA for human (transgenic) IL-1β showed age dependent hIL-1β protein expression levels.

(C) mRNA expression (RT-qPCR) of IL1-receptor-antagonist (*IL1ra*) in different organs in 12-month-old *L2-IL-1β* mice compared to WT littermates.

(D) ELISA for serum levels and organ protein expression of mIL-6 in *L2-IL-1β* mice compared to WT (C57/B6) littermates.

(E) Histopathologic changes in *L2-IL-1β* mice occurred at the squamo-columnar junction (SCJ, arrow in WT). Representative pictures of WT and 6-, 9-, 12-, 15-, and 20-month-old *L2-IL-1β*, top panels show an overview of the SCJ, where the squamous esophagus epithelium meets the columnar cardia/stomach epithelium, second and third panels show inset magnifications of the stepwise progression to BE and EAC.

(F) Histopathologic scoring of 6-, 9-, 12-, 15-, and 20-month-old *L2-IL-1β* mice compared to WT (C57/B6) littermates.

(G) Representative gross pictures of the SCJ in WT and 20 months old *L2-IL-1β* mice with tumor (arrow). Data are represented as mean ± SEM. *$p < 0.05$, **$p < 0.01$. See also Figure S1.

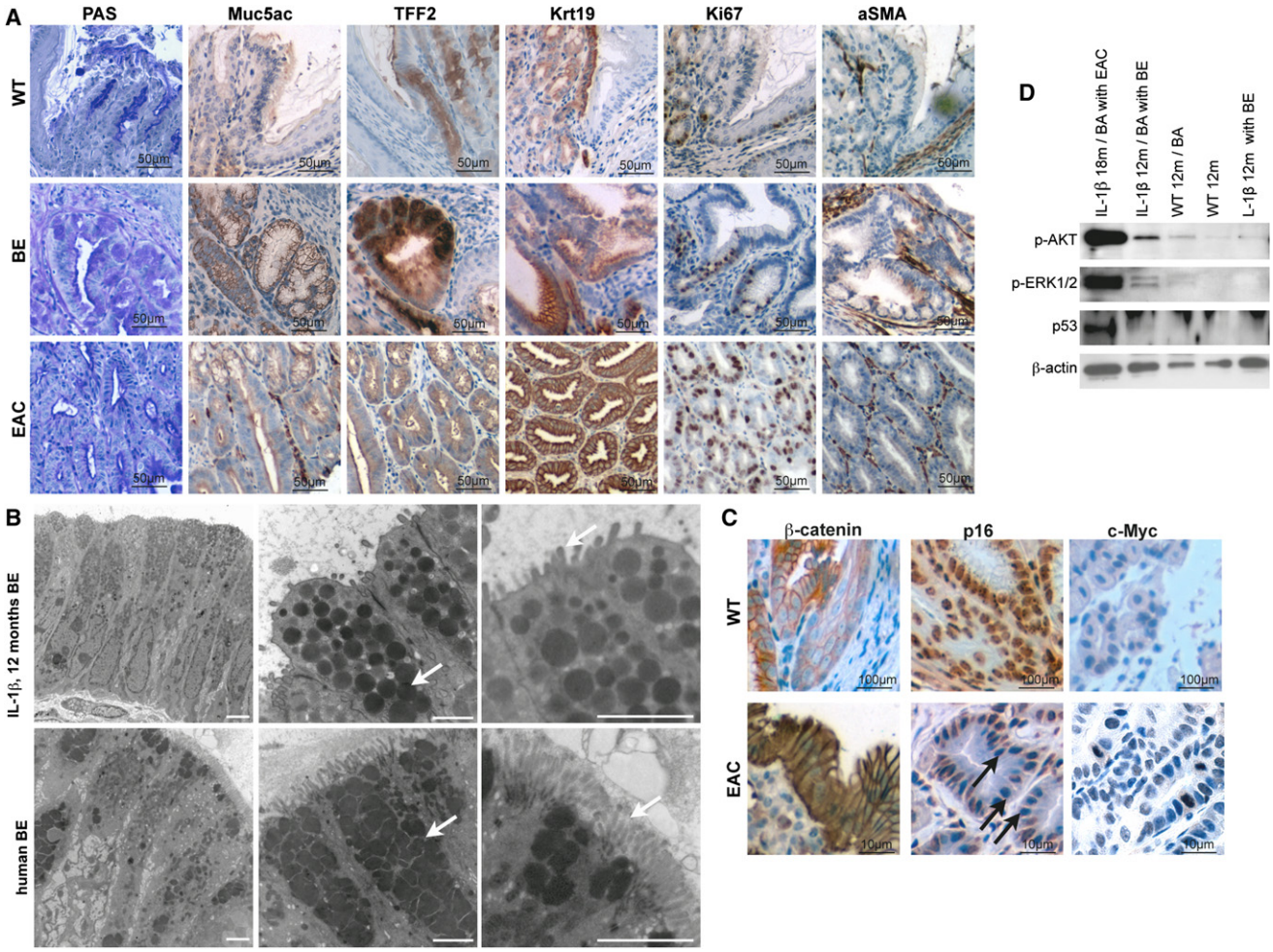

Figure 2. IL-1β Mouse Model Resembles the Human Disease

(A) Representative pictures of staining for PAS, Muc5ac, Krt19, Tff2, Ki67, and αSma of normal SCJ histology in WT (left panel), BE histology in 15-month-old *L2-IL-1*β mice (middle panel), and HGD histology in 22-month-old *L2-IL-1*β mice (right panel).

(B) Representative electron microscopy pictures of mouse (top panel) human (bottom panel) BE epithelium showing columnar cells (left), granules with mucin (middle), and microvilli (right). Scale bar represents 2 μm.

(C) Representative pictures of β-catenin, p16 and c-*myc* in WT mice and dysplastic tissue of 16-month-old BA-treated *L2-IL-1*β mice.

(D) Western blot for p53, p-Erk, and p-Akt in indicated tissues, showing p53 stabilization, and activation of Akt and Erk pathways in EAC- and BA-treated BE. See also Figure S2 and Table S1.

indeed suspect) gene specific hypermethylation in epithelial cells as described in humans (Sato and Meltzer, 2006).

Within the epithelial compartment, we observed stabilization of nuclear β-catenin (Figure 2C), a finding suggested by gene expression microarrays of WT and HGD tissue following laser capture microdissection (LCM) of metaplastic lesions in *L2-IL-1*β mice (Table S1). This microarray analysis confirmed an upregulation of β-*catenin*, *EVI1*, and *RRas* in the tumors, consistent with activation of these pathways. Pathway analysis also revealed markedly increased phosphorylation of Akt and Erk in HGD samples (Figure 2D), compared to only a slight increase in BE-like metaplasia, especially after bile acid treatment, and absent expression in WT cardia tissue (Figure 2D). We also observed occasional loss of p16 and increased c-Myc expression or stabilization of p53 in the neoplastic epithelium (Figures 2C and 2D), thus demonstrating involvement in our mouse model of BE/EAC of a number of pathways relevant to human BE and EAC.

Bile Acids and Carcinogens Accelerate the Development of Barrett-Like Metaplasia and Dysplasia that Can Be Diagnosed Endoscopically in the Mouse

BE and EAC have been attributed to acid reflux leading to chronic esophagitis. In our mouse model of chronic inflammation, Barrett-like metaplasia and dysplasia appeared to be more dependent upon IL-1β overexpression than acid exposure, because both WT mice and *L2-IL-1*β mice were kept on acidified water (pH $\leq$ 2.0) but pathological changes were evident only in the *EL2-IL-1*β mice. Unconjugated bile acids are another component of gastroduodenal reflux that has been linked to the development of BE. Consequently, we treated 2–3-month-old *L2-IL-1*β mice (line 2) and WT littermates with an unconjugated

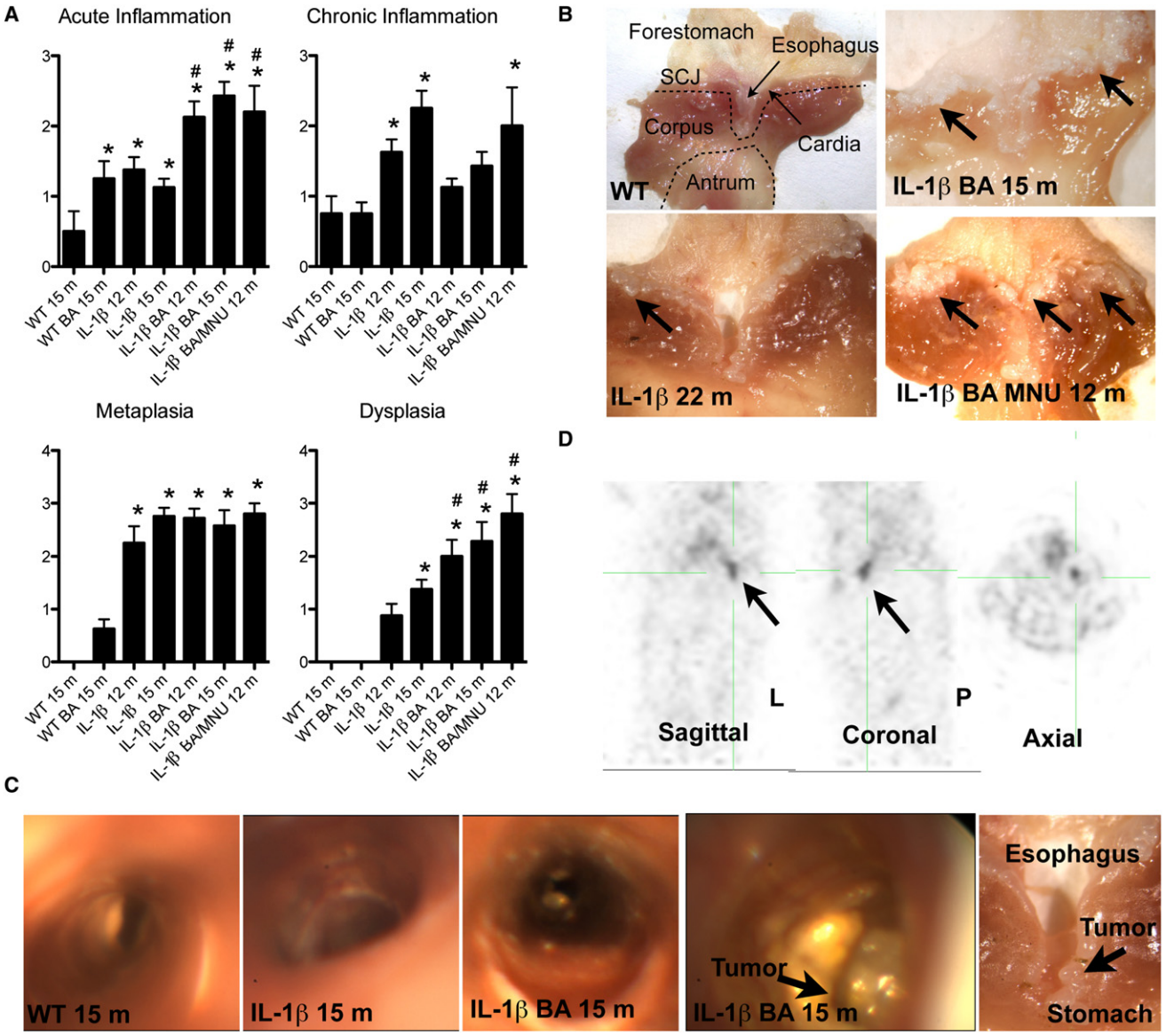

Figure 3. Bile Acids and Carcinogens Accelerate the Development of Barrett Metaplasia and Dysplasia

(A) Histopathological scoring of 6-, 9-, 12-, and 15-month-old BA-treated *L2-IL-1*β mice and combined 12 months old BA and N-methyl-N-nitrosourea (MNU)-treated *L2-IL-1*β mice compared to WT (C57/B6) littermates (*$p < 0.05$ compared to WT, #$p < 0.05$ compared to untreated *L2-IL-1*β mice).

(B) Representative gross pictures of the SCJ in WT, 22-month-old *L2-IL-1*β mice, 15-month-old BA-treated *L2-IL-1*β mice, and combined BA and MNU-treated 12-month-old *L2-IL-1*β mice with tumors at the SCJ.

(C) Representative pictures of the esophagus and SCJ during upper endoscopy in intact 15-month-old BA-treated or untreated *L2-IL-1*β mice and WT mice and corresponding gross macroscopic evaluation (right).

(D) PET imaging was performed on a rodent microPET scanner to measure glucose uptake in tumors relative to normal tissue. A representative picture of 15-month-old BA-treated *L2-IL-1*β mice is shown in sagittal, coronal, and axial position (arrow indicates the tumor that was macroscopically and histologically confirmed). Data are represented as mean ± SEM. See also Movies S1–S5 and Figure S3.

bile acid ([BA], 0.2% deoxycholate) in the drinking water (pH 7) and analyzed the mice at 6, 9, 12, and 15 months (Figure S3A). Due to issues of solubility, BA were administered in pH 7.0 water, thus eliminating the possibility of acid exposure.

Six-month-old BA-treated *L2-IL-1*β mice showed severe esophagitis with inflammatory infiltrates, but only moderate changes were observed in BA-treated WT mice (Figures 3A and 3B). Sixty percent (6/10) of 9-month-old BA-treated *L2-IL-1*β mice showed metaplastic changes at the SCJ, with higher overall metaplasia scores compared to untreated *L2-IL-1*β mice (2.7 versus 1.8, $p < 0.05$) (Figure 3A; Figure S3C), indicating a significant acceleration by BA of Barrett-like metaplasia. Moreover, we observed more severe metaplasia and dysplasia in BA-treated *L2-IL-1*β mice compared to untreated *L2-IL-1*β mice at both 12 months (dysplasia score 2.1 versus 1.0, $p < 0.05$) and 15 months (dysplasia score 2.4 versus 1.4,

$p < 0.01$) (Figure 3A; Figure S3C). Forty percent (4/9) of 15-month-old BA-treated *L2-IL-1β* mice presented with macroscopically visible tumors in the distal esophagus (Figure 3B), and exhibited significant weight loss consistent with partially obstructive lesions. These data suggest that BA play a significant role in the pathogenesis of BE and dysplasia, although we did not use bile acids at pH 2.0 and cannot rule out that gastric acid might also have a role in esophageal carcinogenesis.

N-nitrosamines are generated typically at the SCJ from reduction of salivary nitrite to nitric oxide in response to gastric juice (Winter et al., 2007) and might play a role in the pathogenesis of BE. N-methyl-N-nitrosourea (MNU) is a known gastric carcinogen for mice (Tomita et al., 2011), but does not appear to promote transformation of the noninflamed esophageal epithelium (Figures S3A and S3B). Mucosa that is chronically inflamed is thought to be more sensitive to the effects of luminal carcinogens (Winter et al., 2007). Thus, in comparison to BA+MNU-treated WT mice (Figure S3B), we observed a significant increase in tumor development in 12-month-old BA+MNU-treated *L2-IL-1β* mice (Figures 3A and 3B).

Patients with EAC lose weight due to luminal obstruction, typically diagnosed by endoscopy and/or noninvasive imaging. Upper endoscopy in intact 15-month-old BA-treated or untreated *L2-IL-1β* (Movies S1 and S2) and WT (Movie S3) mice after intubation and under constant ventilation (Figure 3C) revealed the luminal presence of BE-like metaplasia and tumor growth in the distal esophagus. The esophagi of *L2-IL-1β* mice showed circumferential erythema and edema with inflammatory exudates compared to the normal esophagus (Figure 3C), changes that were increased in BA-treated *L2-IL-1β* mice. The endoscopic appearance resembled human BE (Movie S4). In four of nine BA-treated *L2-IL-1β* mice (15 month) but no *L2-IL-1β* mice (15 month), we observed obstructing tumors at the SCJ (Figure 3C; Movies S1–S3). 18F-FDG PET scans of BA-treated *L2-IL-1β* mice with endoscopically detected tumors revealed markedly increased focal glucose uptake, consistent with the severe inflammation in the esophagus and forestomach, along with tumorigenesis confirmed histologically (Figure 3D; Movie S5). These imaging data provide support for the acceleration of neoplastic processes in *L2-IL-1β* mice by BA.

Bile Acids Induce an Acute and Chronic Immune Response and Activate Differential Gene Expression in BE

Previous studies of IL-1β-induced carcinogenesis suggested that recruitment of myeloid cells is crucial for the development of neoplasia (Tu et al., 2008; Yang et al., 2011). In 6-month-old *L2-IL-1β* mice with mild esophagitis, there was no change in the abundance of $CD4^+$ and $CD8^+$ T cells or $CD11b^+/F4/80^+$ monocytes/macrophages in esophageal tissue, but a significant accumulation of immature ($CD11b^+Gr1^+$) myeloid cells (Figure 4C). At 9, 12, and 15 months, there was an even greater accumulation in *L2-IL-1β* mice of $CD11b^+Gr1^+$ cells in the esophagus (Figure 4C) and spleen (not shown) associated with chronic esophagitis and metaplasia. $CD4^+$ T cells, $F4/80^+$ macrophages and $CD11b^-Gr1^+$ neutrophils were also significantly increased but to a lesser extent in *L2-IL-1β* mice at these later time points (Figure 4B). Inflammatory cytokines were increased (Figures 1A–1D; Figure S1D) and the *L2-IL-1β* mice developed splenomegaly, likely due to an accumulation of immature splenic myeloid cells (Figure S1C). BA treatment resulted in additional increases in $CD4^+$ T cells and $CD11b^-Gr1^+$ neutrophils, along with a slight decrease in $CD11b^+Gr1^+$ cells but no changes in $CD11b^+/F4/80^+$ macrophages (Figures 4A and 4B). These observations confirmed our histopathological scoring, showing more acute inflammation in BA-treated mice (Figure 3A). Our data suggest that BA may contribute to the development of BE by shifting the chronic inflammatory response toward an acute neutrophilic response. Recruited macrophages also suggest a role for tumor associated macrophages (TAMs) in BE.

In addition, 15 month BA-treated *L2-IL-1β* mice harboring metaplasia showed elevated levels of *Tff2*, *Cckbr*, *Muc5ac*, *Cdx2*, and *Krt19* (Figure 4D). *Bmp4*, *Cdx2*, and *Shh*, which are known to be involved in cellular differentiation and proliferation, were also associated with BA treatment (Figure 4D). Interestingly, we observed a significant upregulation of *Notch1* upon BA treatment, indicating a potentially important role for the Notch signaling pathway in BE and HGD (Figure 4D).

DLL1-Dependent Notch Signaling Regulates Differentiation and Correlates with Progression

Notch signaling is an essential factor in intestinal differentiation and seems to be required to maintain stem cells in an uncommitted state (Kim and Shivdasani, 2011). As with the intestinal epithelium, the Barrett epithelium contains proliferative crypt-like compartments, and the Notch pathway has been found to be active in BE (Menke et al., 2010). Indeed, *Notch1* was upregulated significantly in the epithelium at the SCJ of BA-treated *L2-IL-1β* mice, compared to WT and untreated *L2-IL-1β* mice (Figures 4D and 5A; Figure S4A), pointing to a role of Notch signaling during EAC pathogenesis. Notch inhibition by systemic treatment with a γ-secretase inhibitor (DBZ), as reported previously (Menke et al., 2010), markedly increased both PAS^+ cells and Alcian-Blue(+) goblet-like cells (Figures 5B and 5C), suggesting that inhibition of Notch signaling is associated with IM. Moreover, IHC for a general marker of activated Notch signaling (Notch intracellular domain or NICD; Figure S4A) revealed that NICD-expressing cells were predominantly found within columnar-lined esophagus (CLE) and dysplastic epithelial tissue at the SCJ, but not in IM at the SCJ, and were in general not present in DBZ-treated mice (Figure 5A; Figure S4A) where we observed increased numbers of goblet cells (Figure 5C). These findings suggest that Notch signaling might contribute to the development of dysplasia, whereas inhibition of Notch signaling results in goblet cell differentiation and may prevent malignant transformation, although in theory both processes could occur simultaneously in different regions of the metaplastic epithelium.

We also observed upregulation of the Notch ligand Delta-like1 (*Dll1*) in BE-like tissue (Figure 5D; Figures S4C and S4D), which correlated with increased Notch1 expression and proliferation in BE. Increasing numbers (Figure S4E) of *Dll1*-expressing cells could be found adjacent to Notch activated cells (Notch-IC), suggesting a possible intraepithelial crosstalk (Figure 5D). Most of the $Dll1^+$ cells also expressed Tff2, supporting a concept of an expansion of Dll^+ cells in the BE lineage (Figure S4F). In addition, we found downregulated Jagged2 gene expression in BE and EAC (Figure 6D; Table S1) and were able to confirm

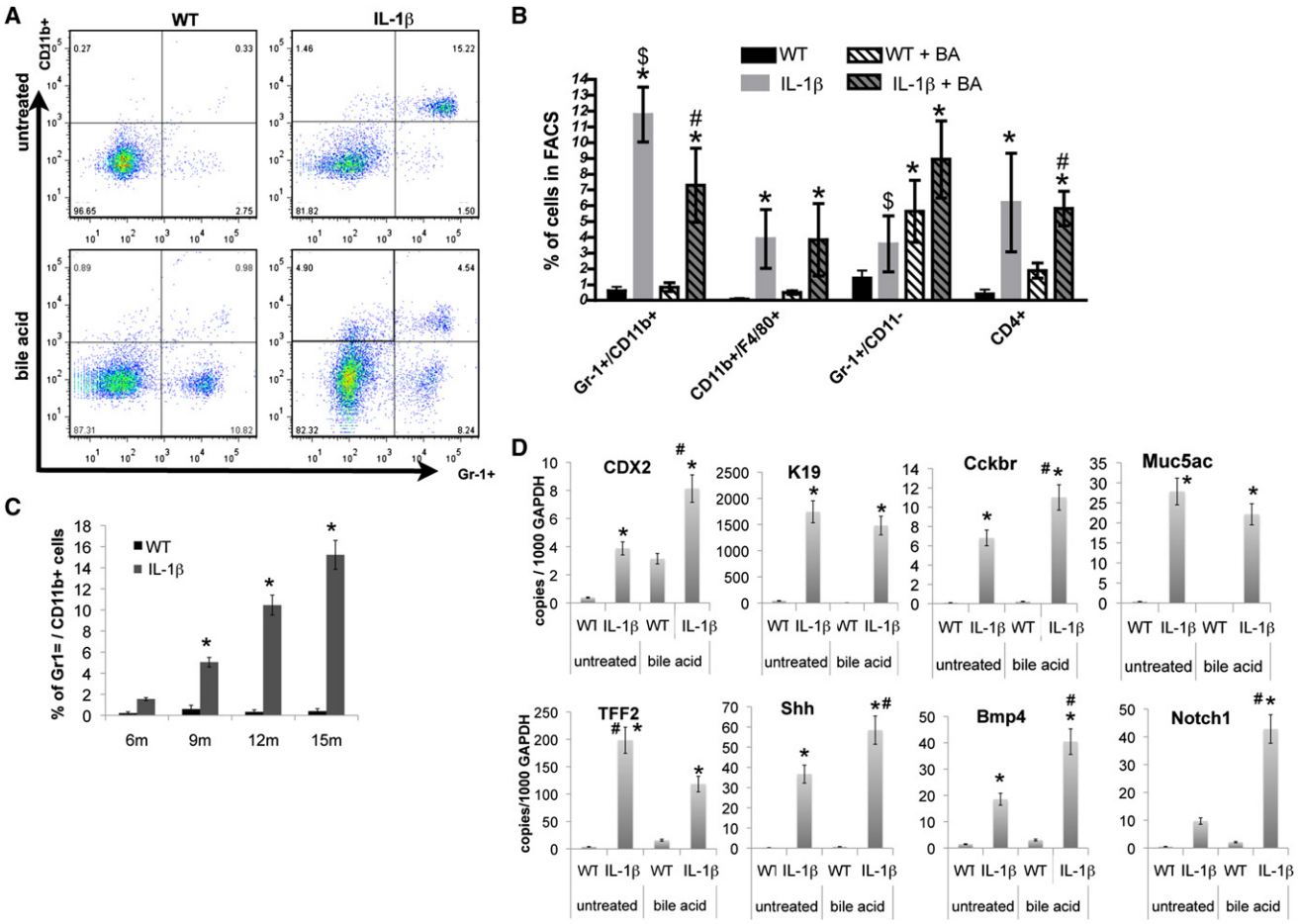

Figure 4. Bile Acids Induce an Acute and Chronic Immune Response and Activate Notch Signaling in BE

(A) The frequencies of lymphoid and myeloid cells in the esophagus from 12-month-old *L2-IL-1β* mice and age-matched WT mice were measured by FACS, and representative FACS blots for detecting immature ($CD11b^+Gr1^+$) myeloid cells in the esophagus from WT, *L2-IL-1β* mice, BA-treated WT, and BA-treated *L2-IL-1β* mice are shown.

(B) Quantitative analysis of FACS for immature ($CD11b^+Gr1^+$) myeloid cells, neutrophiles/granulocytes ($CD11b^-Gr1^+$), macrophages ($Cd11b^+/F4/80^+$), and T cells ($CD4^+$) (*$p < 0.05$ compared to WT, #$p < 0.05$ compared to BA-treated WT, \$$p < 0.05$ compared to untreated *L2-IL-1β* mice).

(C) Quantitative analysis of FACS for immature ($CD11b^+Gr1^+$) myeloid cells in 6-, 9-, 12-, 15-month-old *L2-IL-1β* mice compared to age-matched WT mice.

(D) mRNA expression (RT-qPCR) of Cdx2, K19, Cckbr, Muc5ac, TFF2, Shh, Bmp4, and Notch1 in the SCJ tissue of WT, *L2-IL-1β* mice, BA-treated WT, and BA-treated *L2-IL-1β* mice (*$p < 0.01$ compared to WT, # $p < 0.05$ compared to *L2-IL-1β* mice). Data are represented as mean ± SEM.

decreased Jagged2 as assessed by IHC (Figure S4B), suggesting that Dll1, not Jagged2, is the predominant ligand inducing Notch signaling in BE. The location of Dlll1 expression was associated with the normal stem cell zone in the gastric cardia (data not shown), whereas Jagged2 appeared to be expressed in more terminally differentiated areas of the gastric cardia glands (Figure S4B, data not shown).

To confirm these findings from our mouse model, we analyzed 46 human BE biopsy samples. Biopsies were taken from Barrett mucosa, evaluated by an expert gastrointestinal pathologist, and samples were classified histologically based on the highest degree of neoplasia present on any of the biopsies. *Notch1* was significantly upregulated in human biopsies of dysplastic tissues compared to BE tissue (Figure 5E), pointing to a role of Notch signaling in the development of EAC from BE. Overall, Notch activation appears to be associated with decreased goblet cell differentiation, as suggested by a lack of goblet cells in adjacent tissue of human EAC samples (unpublished data) and a review of the literature (Table S2). IHC for Notch intracellular domain (NICD) and Dll1 in human BE tissue showed a similar pattern, where expression of the receptor and ligand was found in adjacent but distinct cell types (Figure 5F).

Gene Expression Profiles of the IL-1β Mouse Esophagus Closely Resemble Those of Human Barrett Metaplasia and Esophageal Adenocarcinoma

The gene expression profile of human BE (Stairs et al., 2008) is only slightly more similar to small intestine than it is to normal esophagus, in contrast to the striking similarity of BE morphology to intestinal morphology. Nevertheless, we found in both human BE and our mouse model that a number of gastric and intestinal genes were significantly upregulated. LCM was applied to typical metaplastic lesions in *L2-IL-1β* mice (with or without BA), and to the squamous epithelium of WT mice (Figure 6A).

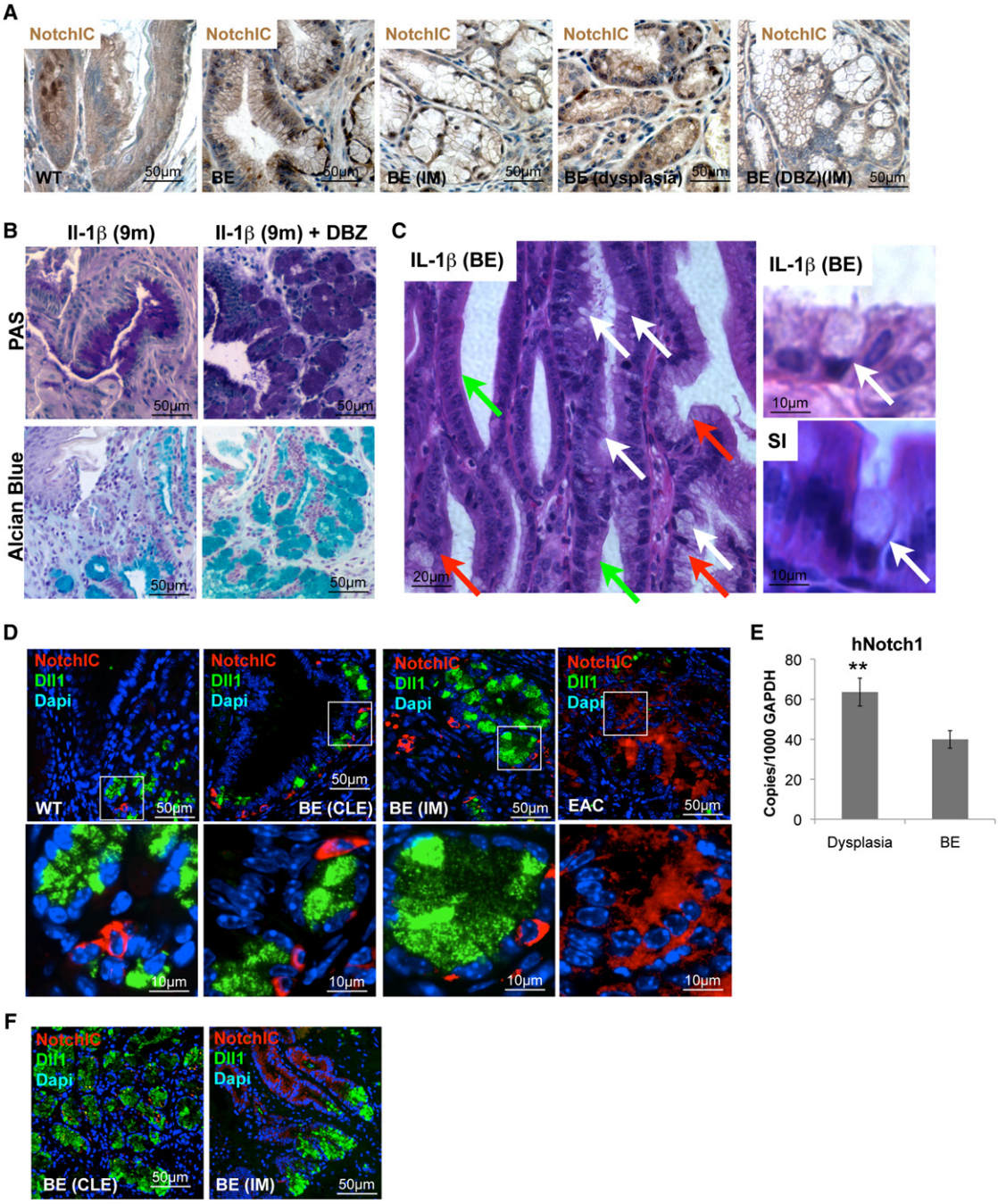

Figure 5. Notch Signaling in BE

(A) Representative pictures of NotchIC IHC in 15-month-old *L2-IL-1*β BA-treated mice and 9-month-old *L2-IL-1*β mice after γ-secretase inhibitor treatment (DBZ).

(B) Representative pictures of periodic acid-Schiff (PAS) and Alcian blue staining at the SCJ of 9-month-old *L2-IL-1*β without and with 10 days γ-secretase inhibitor treatment (right, Notch signaling inhibitor, DBZ).

(C) Representative picture of BE in γ-secretase-treated *L2-IL-1*β mice showing occasional true goblet cells (white arrows), CLE (green arrows), and goblet like cells (red arrows) on the left. On the right goblet cells in BE (top) and small intestine (SI, bottom) are shown to show similarities in intestinal metaplasia.

(D) Representative pictures of NotchIC (red) and Delta-Like1 (Dll1) (green) IHC in 9-month-old WT, 9-month-old *L2-IL-1*β with BE, and 15-month-old BA-treated *L2-IL-1*β with EAC (insets label magnified area below).

(E) mRNA expression (RT-qPCR) of *Notch1* in biopsies of esophageal tissue, obtained from 46 patients with BE with and without dysplasia. In each patient, biopsies were taken from Barrett mucosa and from dysplastic appearing mucosa.

(F) Representative pictures of NotchIC (red) and Delta-Like1 (Dll1) (green) IHC in human BE with CLE or IM. See also Figure S4 and Table S2. Data are represented as mean ± SEM. *$p < 0.05$.

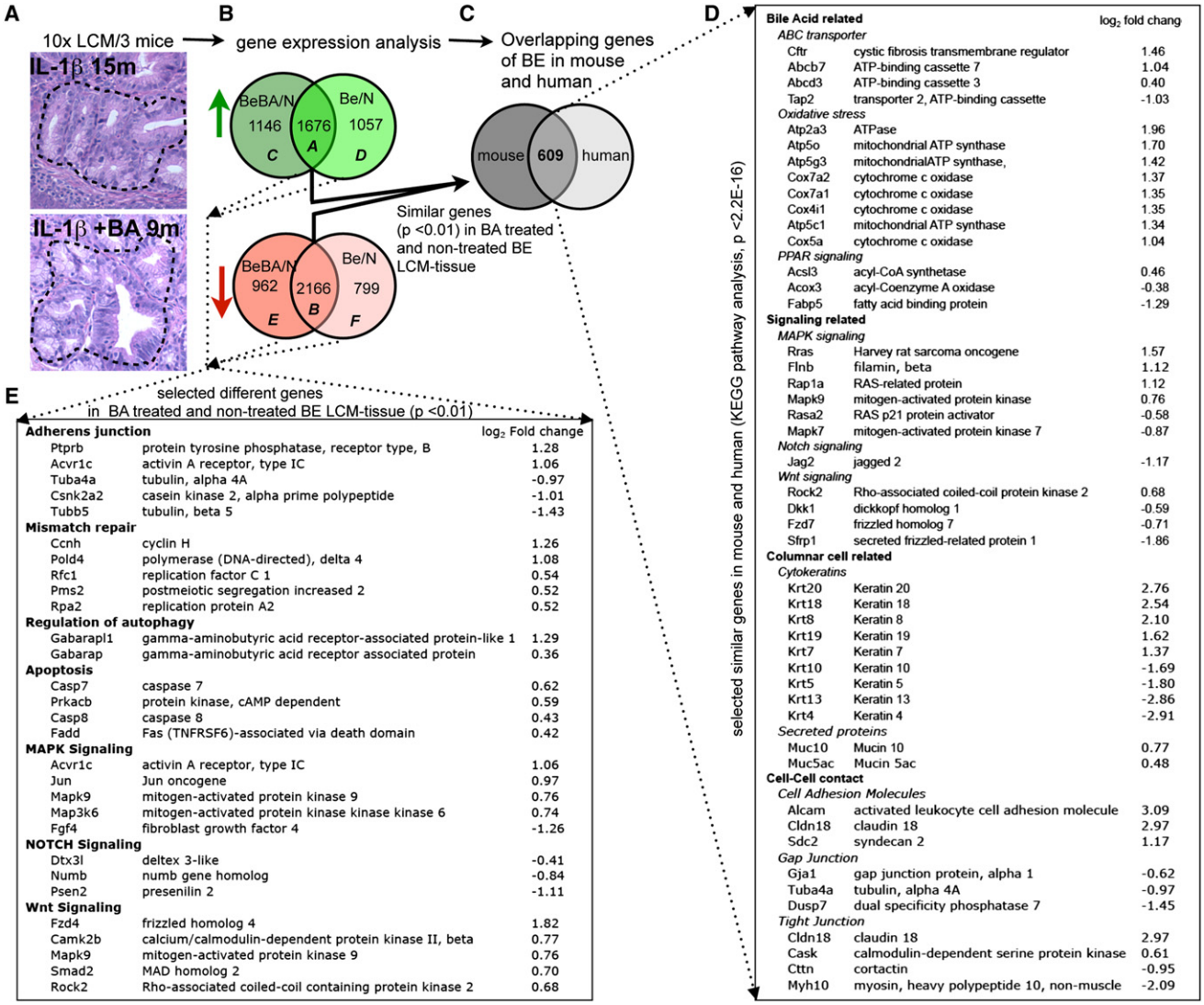

Adherens junction		log2 Fold change
Ptprb	protein tyrosine phosphatase, receptor type, B	1.28
Acvr1c	activin A receptor, type IC	1.06
Tuba4a	tubulin, alpha 4A	-0.97
Csnk2a2	casein kinase 2, alpha prime polypeptide	-1.01
Tubb5	tubulin, beta 5	-1.43
Mismatch repair		
Ccnh	cyclin H	1.26
Pold4	polymerase (DNA-directed), delta 4	1.08
Rfc1	replication factor C 1	0.54
Pms2	postmeiotic segregation increased 2	0.52
Rpa2	replication protein A2	0.52
Regulation of autophagy		
Gabarapl1	gamma-aminobutyric acid receptor-associated protein-like 1	1.29
Gabarap	gamma-aminobutyric acid receptor associated protein	0.36
Apoptosis		
Casp7	caspase 7	0.62
Prkacb	protein kinase, cAMP dependent	0.59
Casp8	caspase 8	0.43
Fadd	Fas (TNFRSF6)-associated via death domain	0.42
MAPK Signaling		
Acvr1c	activin A receptor, type IC	1.06
Jun	Jun oncogene	0.97
Mapk9	mitogen-activated protein kinase 9	0.76
Map3k6	mitogen-activated protein kinase kinase kinase 6	0.74
Fgf4	fibroblast growth factor 4	-1.26
NOTCH Signaling		
Dtx3l	deltex 3-like	-0.41
Numb	numb gene homolog	-0.84
Psen2	presenilin 2	-1.11
Wnt Signaling		
Fzd4	frizzled homolog 4	1.82
Camk2b	calcium/calmodulin-dependent protein kinase II, beta	0.77
Mapk9	mitogen-activated protein kinase 9	0.76
Smad2	MAD homolog 2	0.70
Rock2	Rho-associated coiled-coil containing protein kinase 2	0.68

Bile Acid related		log2 fold chang
ABC transporter		
Cftr	cystic fibrosis transmembrane regulator	1.46
Abcb7	ATP-binding cassette 7	1.04
Abcd3	ATP-binding cassette 3	0.40
Tap2	transporter 2, ATP-binding cassette	-1.03
Oxidative stress		
Atp2a3	ATPase	1.96
Atp5o	mitochondrial ATP synthase	1.70
Atp5g3	mitochondrialATP synthase,	1.42
Cox7a2	cytochrome c oxidase	1.37
Cox7a1	cytochrome c oxidase	1.35
Cox4i1	cytochrome c oxidase	1.35
Atp5c1	mitochondrial ATP synthase	1.34
Cox5a	cytochrome c oxidase	1.04
PPAR signaling		
Acsl3	acyl-CoA synthetase	0.46
Acox3	acyl-Coenzyme A oxidase	-0.38
Fabp5	fatty acid binding protein	-1.29
Signaling related		
MAPK signaling		
Rras	Harvey rat sarcoma oncogene	1.57
Flnb	filamin, beta	1.12
Rap1a	RAS-related protein	1.12
Mapk9	mitogen-activated protein kinase	0.76
Rasa2	RAS p21 protein activator	-0.58
Mapk7	mitogen-activated protein kinase 7	-0.87
Notch signaling		
Jag2	jagged 2	-1.17
Wnt signaling		
Rock2	Rho-associated coiled-coil protein kinase 2	0.68
Dkk1	dickkopf homolog 1	-0.59
Fzd7	frizzled homolog 7	-0.71
Sfrp1	secreted frizzled-related protein 1	-1.86
Columnar cell related		
Cytokeratins		
Krt20	Keratin 20	2.76
Krt18	Keratin 18	2.54
Krt8	Keratin 8	2.10
Krt19	Keratin 19	1.62
Krt7	Keratin 7	1.37
Krt10	Keratin 10	-1.69
Krt5	Keratin 5	-1.80
Krt13	Keratin 13	-2.86
Krt4	Keratin 4	-2.91
Secreted proteins		
Muc10	Mucin 10	0.77
Muc5ac	Mucin 5ac	0.48
Cell-Cell contact		
Cell Adhesion Molecules		
Alcam	activated leukocyte cell adhesion molecule	3.09
Cldn18	claudin 18	2.97
Sdc2	syndecan 2	1.17
Gap Junction		
Gja1	gap junction protein, alpha 1	-0.62
Tuba4a	tubulin, alpha 4A	-0.97
Dusp7	dual specificity phosphatase 7	-1.45
Tight Junction		
Cldn18	claudin 18	2.97
Cask	calmodulin-dependent serine protein kinase	0.61
Cttn	cortactin	-0.95
Myh10	myosin, heavy polypeptide 10, non-muscle	-2.09

Figure 6. Gene Expression Profiles of Mouse BE Resembles that of the Human Disease

(A) Laser capture microdissection (LCM) was applied to typical metaplastic lesions at the SCJ in 15-month-old *L2-IL-1*β mice or 9-month-old BA-treated *L2-IL-1*β mice and to the squamous epithelium of WT control mice. A schematic sequence of the experimental procedures is shown: (A) After LCM (a representative outlined area is shown) followed by RNA isolation and amplification, (B) Venn diagram mouse BE versus BA-treated mouse BE: gene expression of BE tissue from untreated *L2-IL-1*β mice (n = 3, BE versus N), and BA-treated *L2-IL-1*β mice (n = 3, BeBA versus N) was compared to WT squamous tissue (n = 3) in order to determine the overlapping up- and downregulated genes in both cohorts.

(C) Venn diagram mouse versus human. These 3,832 significantly different genes (1,676 up [Venn diagram: A] and 2,166 down [Venn diagram: B], $p < 0.01$) were than compared to the gene expression pattern of a human expression analysis (Stairs et al., 2008) where human BE tissue was compared to human esophageal squamous tissue. This comparison identified 606 genes, which were analyzed by KEGG pathway analysis.

(D) A list of these significantly identical genes in human and mouse is shown with the $\log_2$ fold change of the comparison of BA-treated *L2-IL-1*β mice compared to the squamous epithelium of WT control mice.

(E) KEGG pathway analysis also identified genes that were altered differentially in BE epithelium of *L2-IL-1*β mice versus BA-treated *L2-IL-1*β mice (Venn diagram: C–F). A list of significantly different genes is shown.

Compared to squamous epithelium, we observed 5,698 genes with a significance cutoff of <0.05, that were differentially regulated in BE tissue of 15-month-old *L2-IL-1*β mice and 5,950 genes in 9-month-old BA-treated *L2-IL-1*β mice. Direct comparison of these two groups identified 1,678 similarly upregulated (A in Venn diagram) and 2,166 similarly downregulated (B in Venn diagram) genes (Figure 6B). In KEGG pathway analysis, these transcripts were enriched for cell adhesion molecules, adherens junctions, tight junctions, biosynthesis of unsaturated fatty acids, PPAR signaling pathway, and protein export. When compared to the earlier human expression analysis (GSE13083) (Stairs et al., 2008), entire sets of genes in the mouse were altered in the same directions (Figure 6C). KEGG pathway analysis of those genes that were identically up- or downregulated in mouse and human, revealed changes in the expression of genes relevant for bile acid-induced

damage, signaling pathways (i.e., Notch), columnar cell related genes, and cell-cell contact genes (Figure 6D).

KEGG pathway analysis also identified genes that were altered differentially in BE-like epithelium of *L2-IL-1β* mice versus BA-treated *L2-IL-1β* mice (C–F in Venn diagram) with a significant overrepresentation of the biological processes of mismatch repair, adherens junction, apoptosis, and autophagy, as well as alterations in signaling pathways with importance for carcinogenesis (Figure 6E). These results are consistent with a role for bile acids in promoting metaplasia and cancer by loosening cell-cell contacts, inducing oncogenic pathways, and causing cell death by DNA damage and oxidative stress.

Barrett-Like Metaplasia and Dysplasia Correlate with Expansion of Gastric Cardia Progenitor Cells in Mice and Humans

The current paradigm suggests that BE derives from dedifferentiation or transdifferentiation of the squamous esophageal epithelium (Jankowski et al., 2000). To address the possible origins of BE in our mouse model, we examined the expression and localization of a number of putative stem cell or progenitor cell markers. Lgr5/GPR49 is a validated stem or progenitor cell marker for the mouse gut, but in the stomach it is expressed only in the gastric antrum and in the gastric cardia (Barker et al., 2010). Krt19 and Tff2 have been shown through lineage tracing studies to label different gastric progenitor cells (Means et al., 2008; Quante et al., 2010). Doublecortin and CaM like-kinase-1 (Dclk1), a microtubule-associated kinase expressed in neurons, has been postulated to be expressed in gut epithelial progenitors (Giannakis et al., 2006).

Although the above markers were absent from the normal squamous esophageal epithelium, they showed increased expression over time in our *L2-IL-1β* mouse model, with expression first in the gastric cardia and later above the SCJ. In qRT-PCR studies Lgr5 was expressed minimally in the WT cardia, but could easily be detected in the cardia in 15-month-old *L2-IL-1β* mice that showed features consistent with Barrett metaplasia (Figure 7B). Lgr5-labeled cells were present in the cardia of Lgr5-Cre-ERT mice crossed to Rosa-LacZ reporter mice shortly after tamoxifen induction, which within 7 days gave rise to lineage traced cardia epithelium in WT mice (Figure 7D), as previously shown (Barker et al., 2010). In *L2-IL-1β* mice crossed to Lgr5-Cre-ERT/Rosa-LacZ mice, we observed labeled BE metaplasia four months after tamoxifen induction followed by BA treatment at the age of 6–8 weeks (Figure 7D). These findings indicate that Lgr5$^+$ cells within the cardia may function as progenitor cells, and thus potentially as the cells of origin for BE and dysplasia. Furthermore, we observed an increase in protein and mRNA expression of the *Krt19* gene (Figures 2A and 4D), which is a known marker for surface mucus and gastric progenitor cells (Brembeck et al., 2001; Means et al., 2008), and of the *Tff2* gene, expressed in gastric and cardia mucus neck and progenitor cells (Quante et al., 2010), but not in the normal esophageal epithelium (Figures 2A and 4D). Finally, we found an accumulation of Dclk1$^+$ cells adjacent to the metaplastic mucus producing cells in BE tissue (Figures 7A and 7B). Dclk1$^+$ cells are typically present as rare scattered cells localized primarily to the isthmus of the gastric glands (data not shown), but Dclk1$^+$ cells are highly abundant in the gastric cardia, particularly just below the SCJ (Figure 7A). The gradual accumulation of Dclk1$^+$ cells just above the SCJ in *L2-IL-1β* mice positively correlated with the development of metaplasia at the SCJ; with progression to dysplasia, Dclk1 expression was downregulated.

In human BE, qRT-PCR analysis showed a highly significant upregulation of *LGR5* and *DCLK1* compared to normal squamous epithelium (Figure 7C). Moreover, IHC for DCLK1 showed increased expression in dysplastic BE and decreased (or absent) expression of DCLK1 in dysplasia or adenocarcinoma (Figure 7A), similar to the observation in *L2-IL-1β* mice. Consistent with previous reports, TFF2 was highly expressed in Barrett mucosa but not in biopsies of squamous esophageal epithelium (data not shown). Interestingly, LGR5 and DCLK1 were significantly elevated in the gastric cardia of BE patients (Figures 7E and 7F). The upregulation of gastric columnar progenitor cells in the region of the cardia and in BE suggest that the metaplastic lineage in BE lesions in mice and humans may derive from a gastric cardia lineage (Figure 4G).

IL-6 Deficiency Abolishes Inflammation, Metaplasia, and HGD in *L2-IL-1β* Mice

IL-1β is upstream of IL-6 and TNF-α, which are both upregulated in our models (Figure S1D) and overexpression of IL-1β has been shown to induce tumorigenesis of the stomach (Tu et al., 2008). Persistent activation of the transcription factor signal transducer and activator of transcription-3 (Stat3) occurs in a large number of solid malignancies and supports the proliferation and survival of malignant cells, mostly triggered by an autocrine-paracrine production of IL-6 and family members (Bollrath et al., 2009). We observed elevated IL-6 protein levels in the serum and the SCJ of *L2-IL-1β* mice (Figure 1D), and IL-6 could be upregulated further by BA treatment (Figure 8A). IHC revealed increased pStat3$^+$ cells during the progression from normal esophagus to BE and EAC (Figures 8B and 8C). Interestingly, we observed a significant upregulation of *IL-11Ra* and *Jak2*, and downregulation of *Socs3*, in our microarray analysis (Table S3). Given that we demonstrated increased levels of IL-6 and phosphorylated Stat3 in mouse BE-like and dysplasic tissues, *IL-11Ra* upregulation likely represents an inhibitory feedback mechanism. The finding of SOCS3 downregulation, as demonstrated recently (Watanabe et al., 2007), and increased levels of Jak2 with STAT3 activation, suggest a mechanism by which IL-1β and IL-6 could induce the development of cancer in our mouse model of BE/EAC (Lesina et al., 2011).

In human EAC samples qRT-PCR analysis showed a significant upregulation of IL-6 and IL-1β compared to BE samples (Figures 8D and 8E), supporting our hypothesis that both cytokines play an important role during EAC pathogenesis. When we crossed *L2-IL-1β* mice with *IL-6*$^{-/-}$ mice we observed a complete abolishment of the metaplastic and dysplastic phenotype in homozygous *L2-IL-1β*/IL-6$^{-/-}$ mice, and a partly diminished phenotype with little metaplasia and no dysplasia in heterozygous *L2-IL-1β*/*IL-6*$^{-/+}$ mice (Figure 8F). In *L2-IL-1β*/*IL-6*$^{-/-}$ mice, we observed only a minor inflammatory response, which was increased in *L2-IL-1β*/*IL-6*$^{-/+}$ mice, but no increase in pSTAT3$^+$ cells could be detected (data not shown). These data indicate that IL-1β mediates its carcinogenic effect in part through IL-6,

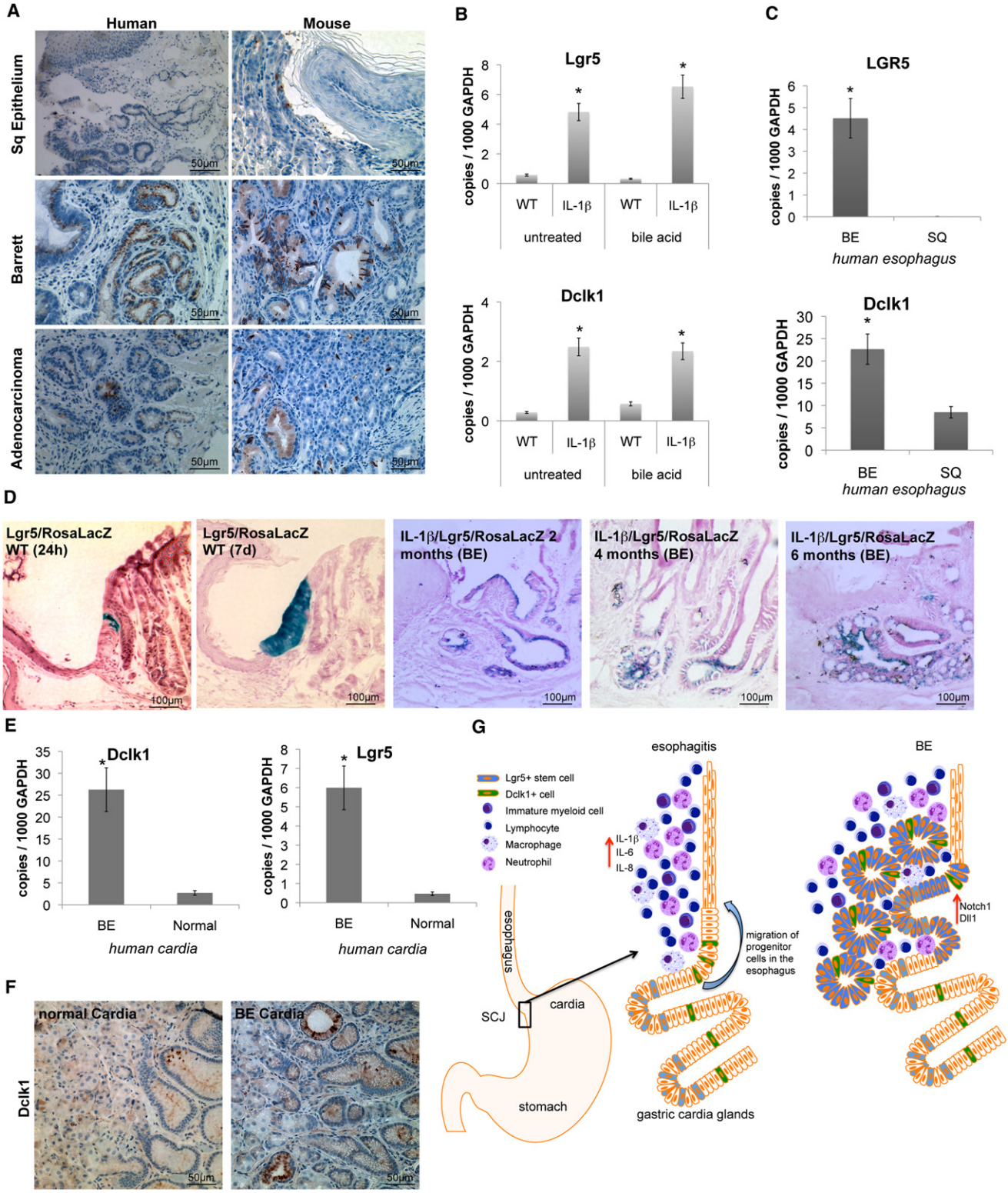

Figure 7. Barrett Metaplasia and Dysplasia Arise from Gastric Cardia Progenitor Cells in Mice and Humans

(A) Representative pictures of human (left) and mouse (right) SCJ, BE, and EAC tissue with doublecortin like kinase-1 (Dclk1) IHC.

(B) mRNA expression (RT-qPCR) of Lgr5 and Dclk1 in the SCJ tissue of WT, *L2-IL-1β* mice, BA-treated WT, and BA-treated *L2-IL-1β* mice.

(C) mRNA expression (RT-qPCR) of *Lgr5* and *Dclk1* in biopsies of esophageal tissue, obtained from 46 patients with BE. In each patient, biopsies were taken from Barrett mucosa and from normal-appearing squamous mucosa.

suggesting the presence of a tumor-promoting IL-1β-IL-6-pStat3 signaling cascade in mouse EAC.

DISCUSSION

Using a transgenic mouse model of esophageal inflammation, we demonstrate that increased IL-1β expression is sufficient for the induction of Barrett-like metaplasia and dysplasia at the SCJ, extending previous findings in the glandular stomach (Tu et al., 2008) and affirming a crucial role for IL-1β in carcinogenesis, which is highly upregulated in human BE and EAC (Fitzgerald et al., 2002). Gene expression analysis, IHC, EM, and endoscopy provided evidence that our IL-1β mouse model closely resembles human disease, despite the fact that the mouse stomach differs from the human stomach. Inflammation in the squamous esophagus resulted in migration of cardia progenitor cells (including $Lgr5^+$ cells) and their metaplastic descendants into the esophagus. We would conclude then that Barrett esophagus is derived from gastric cardia progenitors at the SCJ junction.

Although our L2-IL-1β mouse model exhibits a columnar-lined esophagus (CLE) but lacks abundant goblet cells (or classical IM), it is increasingly recognized that BE does not require classical IM to establish the diagnosis (Ogiya et al., 2008; Playford, 2006). Several studies have indicated that the risk of progression to EAC is the same in patients with CLE without goblet cells as it is in patients with IM (Gatenby et al., 2008; Goldblum, 2010; Kelty et al., 2007; Odze and Maley, 2010; Riddell and Odze, 2009; Takubo et al., 2009) (Table S2), and our clinical experience would support this broader premise. The findings that dysplasia tends to recur following radiofrequency ablation in the presence of CLE without classical IM would support this model (Vaccaro et al., 2011). Notch inhibition has been associated with goblet cell differentiation (Menke et al., 2010), and thus the absence of $Tff3^+$ or $Muc2^+$ goblet cells may be related to the high levels of Notch expression. Our study adds to the evidence challenging the notion that metaplastic nongoblet cell CLE is entirely benign, and we would even argue that TFF2 has many advantages as a marker for BE, because it seems to be expressed early in the development of CLE, a lesion we postulate is the primary precursor lesion for EAC. Nevertheless, further studies in patients are needed to clarify the prognostic and diagnostic value of IM and CLE, because at present it remains controversial as to which metaplastic epithelial subtype best defines BE (Chatelain and Fléjou, 2003), leading to controversial risk estimates for the development of HGD or EAC in BE patients (Hvid-Jensen et al., 2011).

IL-1β overexpression was able to induce metaplasia and dysplasia of the SCJ in part through recruitment of immature myeloid cells (IMC), which have been linked to carcinogenesis (Stairs et al., 2011; Tu et al., 2008; Yang et al., 2011). IMC were increased early in the distal esophagus and likely contribute to esophageal inflammation and carcinogenesis through secretion of pro-inflammatory cytokines (IL-6 and Tnf-α) and chemokines (Sdf1). With BA treatment, there was acceleration of dysplasia and a shift in the myeloid phenotype more toward granulocytic differentiation, pointing to the possible significance of a mixed acute/chronic inflammatory response in carcinogenesis (Fridlender et al., 2009). IL-6 levels were systemically elevated in *L2-IL-1β* mice, and IL-6 deficiency completely abrogated the IL-1β-induced phenotype, indicating the importance of systemic immune activation in the development of neoplasia. Persistent activation of Stat3 through IL-6 additionally supports the proliferation and survival of malignant cells in mouse and human EAC, in contrast to the importance of IL-11 in carcinogenesis of the antrum (Ernst et al., 2008; Howlett et al., 2009). IL-6 in most tissues is a critical mediator of cancer initiation and progression, and IL-6-Stat3 inhibition may be a useful target for prevention or treatment of BE and EAC.

Unconjugated BA, which are increased in the refluxate of patients with BE (Kauer et al., 1997) and in patients on a high fat diet (Theisen et al., 2000), accelerated the development of BE and dysplasia. Unconjugated BA can induce gene promoter demethylation leading to activation of *IL-6*, *Cdx2*, or *Notch1* gene expression in esophageal cells (Jankowski et al., 1999; Kazumori et al., 2006), a finding we can confirm in our BA-treated *L2-IL-1β* mice. Thus, through modulation of gene expression, unconjugated bile acids may promote an intestinal lineage commitment by progenitors. Pathway analysis of our gene expression studies confirm previously suggested carcinogenic roles for BA (Bernstein et al., 2005, 1999; Dvorak et al., 2007; Payne et al., 2005).

Although it is generally accepted that BE and EAC arise from a common progenitor cell, the precise type and location of this cell remained unresolved. Temporal analysis of the *L2-IL-1β* mouse SCJ at different stages of the disease showed an initial expansion of progenitors in the gastric cardia, followed by migration over time into the esophagus (Figure 4G). LgR5 cell lineage tracing studies demonstrated the likely origin of at least some of the metaplastic BE tissue from $Lgr5^+$ cells within the gastric cardia, where $Lgr5^+$ cells also serve as functional cardia stem or progenitor cells. Furthermore, progenitor markers were essentially absent from the normal esophageal squamous epithelium, but Lgr5 (Barker et al., 2010), Tff2 (Quante et al., 2010), Krt19 (Means et al., 2008), Cck2r (Jin et al., 2009), and Dclk1 (Giannakis et al., 2006) were all present in the normal mouse gastric cardia, and were significantly increased in BE. Analysis of a cohort of human patients with BE showed

(D) Left: Lgr5-Cre-ERT x RosaLacZ mice were treated with 3-OH tamoxifen and sacrificed 1 day or 7 days postinduction. Analysis at 1 day showed a small collection of $Xgal^+$ cells in the cardia at the squamocolumnar junction (SCJ), whereas analysis at 7 days showed complete lineage tracing of these columnar cardia glands. Right: lineage tracing of BE tissue in 6-month-old Lgr5-CreERT/IL-1b/RosaLacZ mice. Tamoxifen induction (6 mg in one dose) was performed prior to bile acid treatment at the age of 4 weeks. Mice were sacrificed at 2, 4, or 6 months after induction, indicating lineage tracing of developing BE suggesting that Lgr5 cells might migrate into the distal esophagus and give rise to BE.

(E) mRNA expression (RT-qPCR) of *LGR5* and *DCLK1* in biopsies of cardia tissue, obtained from five patients with BE and five patients without BE (normal).

(F) Representative DCLK1 IHC pictures of normal human cardia (left) and of cardia from patients with BE (right) with doublecortin-like kinase-1.

(G) In our model of the pathogenesis of BE and EAC in mice, bile acid treatment, and IL-1β-induced inflammation lead to migration of gastric cardia progenitor cells into the distal esophagus, giving rise to BE and EAC in association with increased Dll1-dependent Notch signaling that induced columnar cell differentiation.

Data are represented as mean ± SEM. *$p < 0.05$.

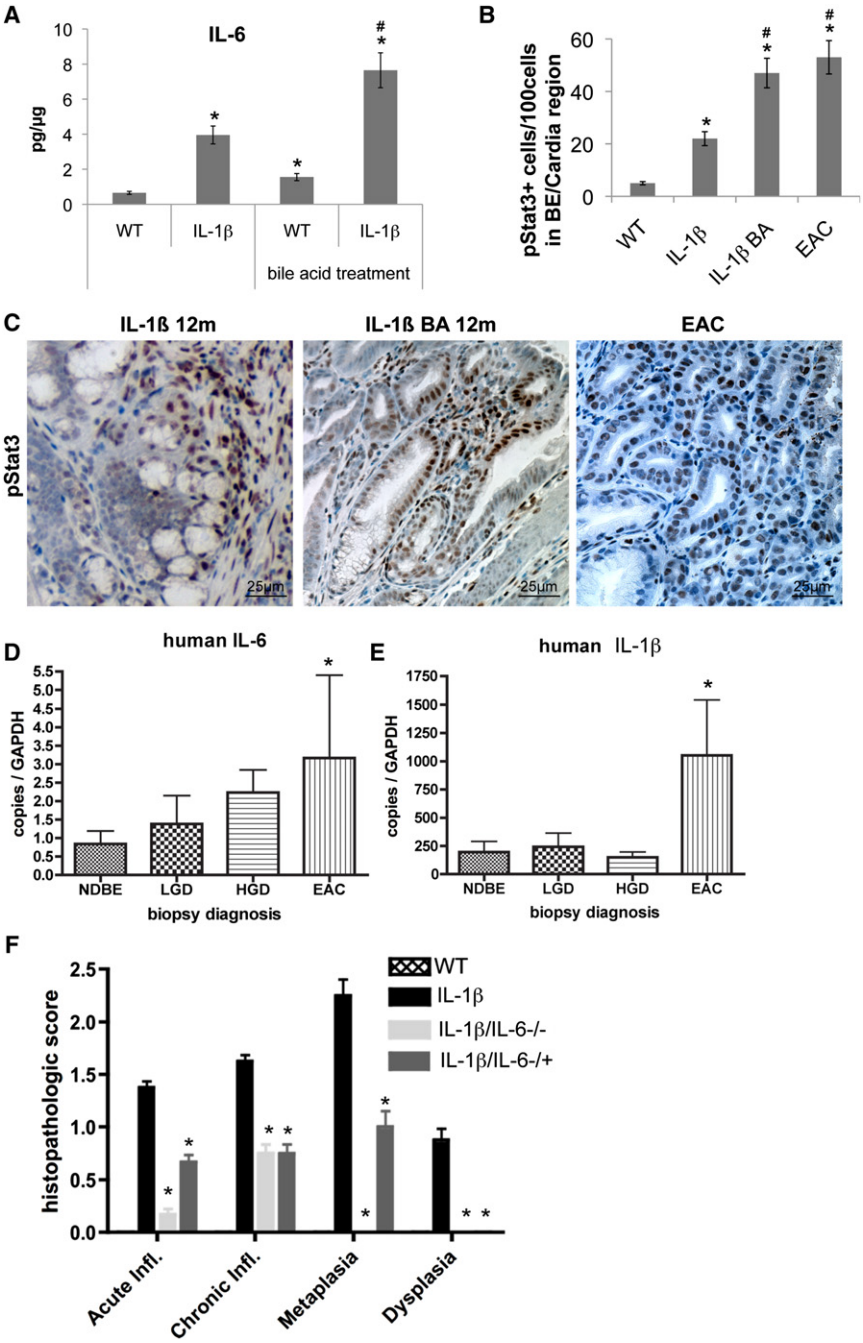

Figure 8. IL-6 Deficiency Abolishes IL-1β-Induced Metaplasia and Dysplasia

(A) mRNA expression (RT-qPCR) of IL-6 in the SCJ tissue of WT, *L2-IL-1β* mice, BA-treated WT, and BA-treated *L2-IL-1β* mice (*p < 0.01 compared to WT, # p < 0.05 compared to *L2-IL-1β* mice).

(B) Quantification of cells with phosphorylated STAT3 in WT, *L2-IL-1β* mice, BA-treated *L2-IL-1β*, and BA-treated *L2-IL-1β* mice with EAC (*p < 0.01 compared to WT, # p < 0.05 compared to *L2-IL-1β* mice).

(C) Representative pictures of pSTAT3 IHC in 12-month-old *L2-IL-1β* mice and BA-treated *L2-IL-1β*, and 15-month-old BA-treated *L2-IL-1β* mice with EAC.

(D and E) mRNA expression (RT-qPCR) of IL-6 (D) and IL-1β (E) in biopsies of esophageal tissue, obtained from 46 patients with BE.

(F) Histopathological scoring of 12-month-old *L2-IL-1β* mice and *L2-IL-1β*/IL-6$^{-/-}$ or *L2-IL-1β*/IL-6$^{-/+}$ mice and WT (C57/B6) littermates (*p < 0.05, compared to *L2-IL-1β* mice). Data are represented as mean ± SEM. See also Table S3.

a significant increase of identical progenitor markers in both gastric cardia and BE tissue.

However, our findings that Lgr5^{+} cardia cells can contribute to BE does not exclude contributions from other lineages. In addition, the use of mouse models to investigate the origins of human metaplasia has its limitations, given the anatomical differences. The predominant theory for the origins of Barrett esophagus is based on the notion of reflux-induced transdifferentiation of squamous epithelial cells (Barbera and Fitzgerald, 2010; Yu et al., 2005). In addition, genetic evidence has supported the possible origin from multipotent progenitors present in submucosal squamous gland ducts, which are not present in the mouse and thus could not be examined in our model (Jankowski et al., 2000; Leedham et al., 2008). A recent study of *p63 null* mice led to the proposal that Barrett-like metaplasia may arise from a population of Car4^{+}/Krt7^{+} embryonic progenitors at the squamocolumnar junction (Wang et al., 2011). However, each of these alternative hypotheses, although reasonable, is also limited to date by the absence of dynamic lineage tracing and the sort of mechanistic underpinnings provided by our model.

Notch signaling appears important in the regulation of stem cell differentiation, and our data suggest that Dll1 is the major ligand inducing activated Notch signaling in BE, whereas Jagged2 may acts as an inhibitor, similar to a model of antagonism between different Notch ligands suggested previously (Benedito et al., 2009). In the cardia, Dll1 was expressed at the bottom of the crypts adjacent to the location of Lgr5 cells. Notch activation in Lgr5^{+} cells has been shown to correlate with lineage tracing at the SCJ at the cardia (Kim and Shivdasani, 2011), consistent with our hypothesis that Lgr5 cells from the gastric cardia migrate into the distal esophagus to give rise to BE tissue with increased Notch activation and Lgr5 expression. With the expansion of progenitor cells in BE, we observe a similar expansion of Dll1^{+} cells immediately adjacent to Notch expressing cells within the metaplastic lineage. The strong correlation between Dll1 with the progenitor cell zone and proliferation, and Jagged2 with postmitotic, differentiated cells, suggests a potential mechanism for modulation of progenitor cell expansion and differentiation through Notch signaling. In this model, Dll1 promotes progenitor

cell maintenance and proliferation, and Jagged2 inhibits proliferation and promotes differentiation, both a consequence of intraepithelial crosstalk between progenitor cells and their progeny. We would further hypothesize, that the development of IM occurs in a low Notch signaling environment, whereas maintenance of the CLE phenotype and progression to dysplasia occurs in a high Notch signaling environment.

Taken together, our data strongly suggest that BE arises from a gastric cardia lineage, as originally suggested (Hamilton and Yardley, 1977). Indeed, it has been difficult to distinguish at the histopathological level between so-called esophagogastric "junctional tumors" that appear localized to the cardia and EAC, clearly present in the esophagus. The fact that BE always begins precisely at the SCJ has never otherwise been explained, and it now seems clear that special consideration should be given to "carditis," inflammation of the gastric cardia that may represent a precursor lesion of BE and EAC.

EXPERIMENTAL PROCEDURES

For a detailed description of all methods see Supplemental Experimental Procedures.

Mice

All mice studies and breeding were carried out under the approval of Institutional Animal Care and Use Committee of Columbia University. Human *IL-1β* transgenic mice were generated by targeting expression of hIL-1β to the esophagus using the Epstein-Bar virus promoter. Mice were placed on drinking water containing bile acids (0.3% DCA, pH 7.0) at the age of 3 months. Nine-month-old L2-IL-1β mice were subjected to a 5-day treatment regimen with the GSI (DBZ, 30 mmol/kg). Lineage tracing studies were performed with Lgr5-CreTM-IRES-GFP mice crossed to Rosa26R-LacZ reporter and L2-IL-1β mice. Tamoxifen (6 mg) was given at the age of 6–8 weeks prior to administration of BA.

Human Study

Esophageal tissue was obtained from 46 patients with BE, with and without dysplasia. Biopsies were taken for clinical and research purposes. This study was approved by the Columbia University Institutional Review Board and informed consent was obtained from all patients.

ACCESSION NUMBERS

Micro array information were deposited at the Gene Expression Omnibus database (http://www.ncbi.nlm.nih.gov/geo/) with the accession number GSE24931.

SUPPLEMENTAL INFORMATION

Supplemental Information includes four figures, three tables, Supplemental Experimental Procedures, and five movies and can be found with this article online at doi:10.1016/j.ccr.2011.12.004.

ACKNOWLEDGMENTS

These studies are supported by NIH (RO1DK060758, 1U54CA126513, and R01CA120979 to T.C.W; 5U01 CA143056 to A.K.R., T.C.W., U.M.). A.K.R. was further supported by NIH P01-CA098101 and P30-DK050306 grants. M.Q. was supported by a grant from the Mildred-Scheel-Stiftung, Deutsche Krebshilfe, Germany. J.A. is supported by a Career Development Award from the NCI (K07 CA132892) and by a Louis V. Gerstner, Jr. Scholars Award. We acknowledge the assistance of the Transgenic Mouse and Genomics Core of the Irving Cancer Research Center at Columbia University, and the Electronic Microscopy Core Facility at the University of Pennsylvania. We thank all members of the Wang lab for fruitful discussions.

Received: January 14, 2011
Revised: June 2, 2011
Accepted: December 1, 2011
Published: January 17, 2012

REFERENCES

Allison, P.R., and Johnstone, A.S. (1953). The oesophagus lined with gastric mucous membrane. Thorax *8*, 87–101.

Barbera, M., and Fitzgerald, R.C. (2010). Cellular origin of Barrett metaplasia and oesophageal stem cells. Biochem. Soc. Trans. *38*, 370–373.

Barker, N., Huch, M., Kujala, P., van de Wetering, M., Snippert, H.J., van Es, J.H., Sato, T., Stange, D.E., Begthel, H., van den Born, M., et al. (2010). Lgr5(+ve) stem cells drive self-renewal in the stomach and build long-lived gastric units in vitro. Cell Stem Cell *6*, 25–36.

Benedito, R., Roca, C., Sörensen, I., Adams, S., Gossler, A., Fruttiger, M., and Adams, R.H. (2009). The notch ligands Dll4 and Jagged1 have opposing effects on angiogenesis. Cell *137*, 1124–1135.

Bernstein, H., Payne, C.M., Bernstein, C., Schneider, J., Beard, S.E., and Crowley, C.L. (1999). Activation of the promoters of genes associated with DNA damage, oxidative stress, ER stress and protein malfolding by the bile salt, deoxycholate. Toxicol. Lett. *108*, 37–46.

Bernstein, H., Bernstein, C., Payne, C.M., Dvorakova, K., and Garewal, H. (2005). Bile acids as carcinogens in human gastrointestinal cancers. Mutat. Res. *589*, 47–65.

Björkdahl, O., Akerblad, P., Gjörloff-Wingren, A., Leanderson, T., and Dohlsten, M. (1999). Lymphoid hyperplasia in transgenic mice over-expressing a secreted form of the human interleukin-1beta gene product. Immunology *96*, 128–137.

Bollrath, J., Phesse, T.J., von Burstin, V.A., Putoczki, T., Bennecke, M., Bateman, T., Nebelsiek, T., Lundgren-May, T., Canli, O., Schwitalla, S., et al. (2009). gp130-mediated Stat3 activation in enterocytes regulates cell survival and cell-cycle progression during colitis-associated tumorigenesis. Cancer Cell *15*, 91–102.

Brembeck, F.H., Moffett, J., Wang, T.C., and Rustgi, A.K. (2001). The keratin 19 promoter is potent for cell-specific targeting of genes in transgenic mice. Gastroenterology *120*, 1720–1728.

Chatelain, D., and Fléjou, J.F. (2003). High-grade dysplasia and superficial adenocarcinoma in Barrett esophagus: histological mapping and expression of p53, p21 and Bcl-2 oncoproteins. Virchows Arch. *442*, 18–24.

Corley, D.A., Kubo, A., Levin, T.R., Block, G., Habel, L., Rumore, G., Quesenberry, C., and Buffler, P. (2009). Race, ethnicity, sex and temporal differences in Barrett oesophagus diagnosis: a large community-based study, 1994-2006. Gut *58*, 182–188.

Dvorak, K., Payne, C.M., Chavarria, M., Ramsey, L., Dvorakova, B., Bernstein, H., Holubec, H., Sampliner, R.E., Guy, N., Condon, A., et al. (2007). Bile acids in combination with low pH induce oxidative stress and oxidative DNA damage: relevance to the pathogenesis of Barrett oesophagus. Gut *56*, 763–771.

Ernst, M., Najdovska, M., Grail, D., Lundgren-May, T., Buchert, M., Tye, H., Matthews, V.B., Armes, J., Bhathal, P.S., Hughes, N.R., et al. (2008). STAT3 and STAT1 mediate IL-11-dependent and inflammation-associated gastric tumorigenesis in gp130 receptor mutant mice. J. Clin. Invest. *118*, 1727–1738.

Falk, G.W. (2002). Barrett esophagus. Gastroenterology *122*, 1569–1591.

Fein, M., Peters, J.H., Chandrasoma, P., Ireland, A.P., Oberg, S., Ritter, M.P., Bremner, C.G., Hagen, J.A., and DeMeester, T.R. (1998). Duodenoesophageal reflux induces esophageal adenocarcinoma without exogenous carcinogen. J. Gastrointest. Surg. *2*, 260–268.

Fitzgerald, R.C., Abdalla, S., Onwuegbusi, B.A., Sirieix, P., Saeed, I.T., Burnham, W.R., and Farthing, M.J. (2002). Inflammatory gradient in Barrett oesophagus: implications for disease complications. Gut *51*, 316–322.

Fox, J.G., Beck, P., Dangler, C.A., Whary, M.T., Wang, T.C., Shi, H.N., and Nagler-Anderson, C. (2000). Concurrent enteric helminth infection modulates inflammation and gastric immune responses and reduces Helicobacter-induced gastric atrophy. Nat. Med. *6*, 536–542.

Fridlender, Z.G., Sun, J., Kim, S., Kapoor, V., Cheng, G., Ling, L., Worthen, G.S., and Albelda, S.M. (2009). Polarization of tumor-associated neutrophil phenotype by TGF-beta: "N1" versus "N2" TAN. Cancer Cell *16*, 183–194.

Gatenby, P.A., Ramus, J.R., Caygill, C.P., Shepherd, N.A., and Watson, A. (2008). Relevance of the detection of intestinal metaplasia in non-dysplastic columnar-lined oesophagus. Scand. J. Gastroenterol. *43*, 524–530.

Giannakis, M., Stappenbeck, T.S., Mills, J.C., Leip, D.G., Lovett, M., Clifton, S.W., Ippolito, J.E., Glasscock, J.I., Arumugam, M., Brent, M.R., and Gordon, J.I. (2006). Molecular properties of adult mouse gastric and intestinal epithelial progenitors in their niches. J. Biol. Chem. *281*, 11292–11300.

Goldblum, J.R. (2010). Controversies in the diagnosis of Barrett esophagus and Barrett-related dysplasia: one pathologist's perspective. Arch. Pathol. Lab. Med. *134*, 1479–1484.

Gough, M.D., Ackroyd, R., Majeed, A.W., and Bird, N.C. (2005). Prediction of malignant potential in reflux disease: are cytokine polymorphisms important? Am. J. Gastroenterol. *100*, 1012–1018.

Grivennikov, S., and Karin, M. (2008). Autocrine IL-6 signaling: a key event in tumorigenesis? Cancer Cell *13*, 7–9.

Grivennikov, S.I., Greten, F.R., and Karin, M. (2010). Immunity, inflammation, and cancer. Cell *140*, 883–899.

Hamilton, S.R., and Yardley, J.H. (1977). Regenerative of cardiac type mucosa and acquisition of Barrett mucosa after esophagogastrostomy. Gastroenterology *72*, 669–675.

Hanby, A.M., Jankowski, J.A., Elia, G., Poulsom, R., and Wright, N.A. (1994). Expression of the trefoil peptides pS2 and human spasmolytic polypeptide (hSP) in Barrett metaplasia and the native oesophageal epithelium: delineation of epithelial phenotype. J. Pathol. *173*, 213–219.

Howlett, M., Giraud, A.S., Lescesen, H., Jackson, C.B., Kalantzis, A., Van Driel, I.R., Robb, L., Van der Hoek, M., Ernst, M., Minamoto, T., et al. (2009). The interleukin-6 family cytokine interleukin-11 regulates homeostatic epithelial cell turnover and promotes gastric tumor development. Gastroenterology *136*, 967–977.

Hvid-Jensen, F., Pedersen, L., Drewes, A.M., Sørensen, H.T., and Funch-Jensen, P. (2011). Incidence of adenocarcinoma among patients with Barrett esophagus. N. Engl. J. Med. *365*, 1375–1383.

Jankowski, J.A., Wright, N.A., Meltzer, S.J., Triadafilopoulos, G., Geboes, K., Casson, A.G., Kerr, D., and Young, L.S. (1999). Molecular evolution of the metaplasia-dysplasia-adenocarcinoma sequence in the esophagus. Am. J. Pathol. *154*, 965–973.

Jankowski, J.A., Harrison, R.F., Perry, I., Balkwill, F., and Tselepis, C. (2000). Barrett metaplasia. Lancet *356*, 2079–2085.

Jiang, L., Gonda, T.A., Gamble, M.V., Salas, M., Seshan, V., Tu, S., Twaddell, W.S., Hegyi, P., Lazar, G., Steele, I., et al. (2008). Global hypomethylation of genomic DNA in cancer-associated myofibroblasts. Cancer Res. *68*, 9900–9908.

Jin, G., Ramanathan, V., Quante, M., Baik, G.H., Yang, X., Wang, S.S., Tu, S., Gordon, S.A., Pritchard, D.M., Varro, A., et al. (2009). Inactivating cholecystokinin-2 receptor inhibits progastrin-dependent colonic crypt fission, proliferation, and colorectal cancer in mice. J. Clin. Invest. *119*, 2691–2701.

Kalabis, J., Oyama, K., Okawa, T., Nakagawa, H., Michaylira, C.Z., Stairs, D.B., Figueiredo, J.L., Mahmood, U., Diehl, J.A., Herlyn, M., and Rustgi, A.K. (2008). A subpopulation of mouse esophageal basal cells has properties of stem cells with the capacity for self-renewal and lineage specification. J. Clin. Invest. *118*, 3860–3869.

Kauer, W.K., Peters, J.H., DeMeester, T.R., Feussner, H., Ireland, A.P., Stein, H.J., and Siewert, R.J. (1997). Composition and concentration of bile acid reflux into the esophagus of patients with gastroesophageal reflux disease. Surgery *122*, 874–881.

Kazumori, H., Ishihara, S., Rumi, M.A., Kadowaki, Y., and Kinoshita, Y. (2006). Bile acids directly augment caudal related homeobox gene Cdx2 expression in oesophageal keratinocytes in Barrett epithelium. Gut *55*, 16–25.

Kelty, C.J., Gough, M.D., Van Wyk, Q., Stephenson, T.J., and Ackroyd, R. (2007). Barrett oesophagus: intestinal metaplasia is not essential for cancer risk. Scand. J. Gastroenterol. *42*, 1271–1274.

Kim, T.H., and Shivdasani, R.A. (2011). Notch signaling in stomach epithelial stem cell homeostasis. J. Exp. Med. *208*, 677–688.

Leedham, S.J., Preston, S.L., McDonald, S.A., Elia, G., Bhandari, P., Poller, D., Harrison, R., Novelli, M.R., Jankowski, J.A., and Wright, N.A. (2008). Individual crypt genetic heterogeneity and the origin of metaplastic glandular epithelium in human Barrett oesophagus. Gut *57*, 1041–1048.

Lesina, M., Kurkowski, M.U., Ludes, K., Rose-John, S., Treiber, M., Kloppel, G., Yoshimura, A., Reindl, W., Sipos, B., Akira, S., et al. (2011). Stat3/Socs3 activation by IL-6 transsignaling promotes progression of pancreatic intraepithelial neoplasia and development of pancreatic cancer. Cancer Cell *19*, 456–469.

Li, Y., and Martin, R.C., 2nd. (2007). Reflux injury of esophageal mucosa: experimental studies in animal models of esophagitis, Barrett's esophagus and esophageal adenocarcinoma. Dis. Esophagus *20*, 372–378.

Means, A.L., Xu, Y., Zhao, A., Ray, K.C., and Gu, G. (2008). A CK19(CreERT) knockin mouse line allows for conditional DNA recombination in epithelial cells in multiple endodermal organs. Genesis *46*, 318–323.

Menke, V., van Es, J.H., de Lau, W., van den Born, M., Kuipers, E.J., Siersema, P.D., de Bruin, R.W., Kusters, J.G., and Clevers, H. (2010). Conversion of metaplastic Barrett epithelium into post-mitotic goblet cells by gamma-secretase inhibition. Dis. Model Mech. *3*, 104–110.

Nakagawa, H., Wang, T.C., Zukerberg, L., Odze, R., Togawa, K., May, G.H., Wilson, J., and Rustgi, A.K. (1997). The targeting of the cyclin D1 oncogene by an Epstein-Barr virus promoter in transgenic mice causes dysplasia in the tongue, esophagus and forestomach. Oncogene *14*, 1185–1190.

Nakanishi, Y., Saka, M., Eguchi, T., Sekine, S., Taniguchi, H., and Shimoda, T. (2007). Distribution and significance of the oesophageal and gastric cardiac mucosae: a study of 131 operation specimens. Histopathology *51*, 515–519.

O'Riordan, J.M., Abdel-Latif, M.M., Ravi, N., McNamara, D., Byrne, P.J., McDonald, G.S., Keeling, P.W., Kelleher, D., and Reynolds, J.V. (2005). Proinflammatory cytokine and nuclear factor kappa-B expression along the inflammation-metaplasia-dysplasia-adenocarcinoma sequence in the esophagus. Am. J. Gastroenterol. *100*, 1257–1264.

Odze, R.D., and Maley, C.C. (2010). Neoplasia without dysplasia: lessons from Barrett esophagus and other tubal gut neoplasms. Arch. Pathol. Lab. Med. *134*, 896–906.

Ogiya, K., Kawano, T., Ito, E., Nakajima, Y., Kawada, K., Nishikage, T., and Nagai, K. (2008). Lower esophageal palisade vessels and the definition of Barrett esophagus. Dis. Esophagus *21*, 645–649.

Payne, C.M., Crowley-Weber, C.L., Dvorak, K., Bernstein, C., Bernstein, H., Holubec, H., Crowley, C., and Garewal, H. (2005). Mitochondrial perturbation attenuates bile acid-induced cytotoxicity. Cell Biol. Toxicol. *21*, 215–231.

Playford, R.J. (2006). New British Society of Gastroenterology (BSG) guidelines for the diagnosis and management of Barrett oesophagus. Gut *55*, 442.

Quante, M., Marrache, F., Goldenring, J.R., and Wang, T.C. (2010). TFF2 mRNA transcript expression marks a gland progenitor cell of the gastric oxyntic mucosa. Gastroenterology *139*, 2018–2027.

Riddell, R.H., and Odze, R.D. (2009). Definition of Barrett esophagus: time for a rethink—is intestinal metaplasia dead? Am. J. Gastroenterol. *104*, 2588–2594.

Sato, F., and Meltzer, S.J. (2006). CpG island hypermethylation in progression of esophageal and gastric cancer. Cancer *106*, 483–493.

Spechler, S.J., Fitzgerald, R.C., Prasad, G.A., and Wang, K.K. (2010). History, molecular mechanisms, and endoscopic treatment of Barrett esophagus. Gastroenterology *138*, 854–869.

Stairs, D.B., Nakagawa, H., Klein-Szanto, A., Mitchell, S.D., Silberg, D.G., Tobias, J.W., Lynch, J.P., and Rustgi, A.K. (2008). Cdx1 and c-Myc foster the initiation of transdifferentiation of the normal esophageal squamous epithelium toward Barrett esophagus. PLoS ONE *3*, e3534.

Stairs, D.B., Bayne, L.J., Rhoades, B., Vega, M.E., Waldron, T.J., Kalabis, J., Klein-Szanto, A., Lee, J.S., Katz, J.P., Diehl, J.A., et al. (2011). Deletion of p120-catenin results in a tumor microenvironment with inflammation and cancer that establishes it as a tumor suppressor gene. Cancer Cell *19*, 470–483.

Takubo, K., Aida, J., Naomoto, Y., Sawabe, M., Arai, T., Shiraishi, H., Matsuura, M., Ell, C., May, A., Pech, O., et al. (2009). Cardiac rather than intestinal-type background in endoscopic resection specimens of minute Barrett adenocarcinoma. Hum. Pathol. *40*, 65–74.

Tatsuta, T., Mukaisho, K., Sugihara, H., Miwa, K., Tani, T., and Hattori, T. (2005). Expression of Cdx2 in early GRCL of Barrett esophagus induced in rats by duodenal reflux. Dig. Dis. Sci. *50*, 425–431.

Theisen, J., Nehra, D., Citron, D., Johansson, J., Hagen, J.A., Crookes, P.F., DeMeester, S.R., Bremner, C.G., DeMeester, T.R., and Peters, J.H. (2000). Suppression of gastric acid secretion in patients with gastroesophageal reflux disease results in gastric bacterial overgrowth and deconjugation of bile acids. J. Gastrointest. Surg. *4*, 50–54.

Tomita, H., Takaishi, S., Menheniott, T.R., Yang, X., Shibata, W., Jin, G., Betz, K.S., Kawakami, K., Minamoto, T., Tomasetto, C., et al. (2011). Inhibition of gastric carcinogenesis by the hormone gastrin is mediated by suppression of TFF1 epigenetic silencing. Gastroenterology *104*, 879–891.

Tu, S., Bhagat, G., Cui, G., Takaishi, S., Kurt-Jones, E.A., Rickman, B., Betz, K.S., Penz-Oesterreicher, M., Bjorkdahl, O., Fox, J.G., and Wang, T.C. (2008). Overexpression of interleukin-1beta induces gastric inflammation and cancer and mobilizes myeloid-derived suppressor cells in mice. Cancer Cell *14*, 408–419.

Vaccaro, B.J., Gonzalez, S., Poneros, J.M., Stevens, P.D., Capiak, K.M., Lightdale, C.J., and Abrams, J.A. (2011). Detection of intestinal metaplasia after successful eradication of Barrett Esophagus with radiofrequency ablation. Dig. Dis. Sci. *56*, 1996–2000.

Van De Bovenkamp, J.H., Korteland-Van Male, A.M., Warson, C., Büller, H.A., Einerhand, A.W., Ectors, N.L., and Dekker, J. (2003). Gastric-type mucin and TFF-peptide expression in Barrett oesophagus is disturbed during increased expression of MUC2. Histopathology *42*, 555–565.

Wang, X., Ouyang, H., Yamamoto, Y., Kumar, P.A., Wei, T.S., Dagher, R., Vincent, M., Lu, X., Bellizzi, A.M., Ho, K.Y., et al. (2011). Residual embryonic cells as precursors of a Barrett-like metaplasia. Cell *145*, 1023–1035.

Warson, C., Van De Bovenkamp, J.H., Korteland-Van Male, A.M., Büller, H.A., Einerhand, A.W., Ectors, N.L., and Dekker, J. (2002). Barrett esophagus is characterized by expression of gastric-type mucins (MUC5AC, MUC6) and TFF peptides (TFF1 and TFF2), but the risk of carcinoma development may be indicated by the intestinal-type mucin, MUC2. Hum. Pathol. *33*, 660–668.

Watanabe, F., Iwasaki, Y., Ohashi, M., Nunobe, S., Iwagami, S., Takahashi, K., Yamaguchi, T., Matsumoto, H., and Yasutome, M. (2007). [A case report-the marked response to S-1 + CDDP chemotherapy for post-operative local recurrence of advanced gastric cancer]. Gan To Kagaku Ryoho *34*, 1970–1972.

Winter, J.W., Paterson, S., Scobie, G., Wirz, A., Preston, T., and McColl, K.E. (2007). N-nitrosamine generation from ingested nitrate via nitric oxide in subjects with and without gastroesophageal reflux. Gastroenterology *133*, 164–174.

Yang, X.D., Ai, W., Asfaha, S., Bhagat, G., Friedman, R.A., Jin, G., Park, H., Shykind, B., Diacovo, T.G., Falus, A., and Wang, T.C. (2011). Histamine deficiency promotes inflammation-associated carcinogenesis through reduced myeloid maturation and accumulation of CD11b+Ly6G+ immature myeloid cells. Nat. Med. *17*, 87–95.

Yu, W.Y., Slack, J.M., and Tosh, D. (2005). Conversion of columnar to stratified squamous epithelium in the developing mouse oesophagus. Dev. Biol. *284*, 157–170.